Closed-Loop Extracellular Stimulation of Place Cells in Freely Moving Rats

Dejana Mitrovic

Thesis submitted for the degree of
Master in Molecular Biosciences
(Physiology)
60 credits

Department of Biosciences
Faculty of mathematics and natural sciences

UNIVERSITY OF OSLO

Autumn 2019

Closed-Loop Extracellular Stimulation of Place Cells in Freely Moving Rats

Dejana Mitrovic

Closed-Loop Extracellular Stimulation of Place Cells in Freely Moving Rats

http://www.duo.uio.no/

Printed: Reprosentralen, University of Oslo

Acknowledgements

The project that is being presented in this thesis was performed at the physiology program at the Department of Biosciences, University of Oslo, under the supervision of professor Dr. Marianne Fyhn, and associate professor Dr. Torkel Hafting.

I would like to thank Marianne for believing in me while I was a bachelor's student, and giving me an early opportunity to experience neuroscience while still being an undergraduate. I would also like to thank Torkel for giving me the insight into being a better researcher, and writer. My co-supervisors Alessio Buccino and Malin Benum Røe for the countless hours they spent on assisting me with experiments, analysis, and writing; you have been with me all the way. I am eternally thankful. To my peer and soulmate Can H. Tartanoglu for always assisting me in both academic and personal straits, and for always believing in me. My co-workers at the Center for Integrative Neuroplasticity, thank you for the support, especially Tristan Manfred Stöber. I would also like to thank my study advisor Torill Rørtveit, and my previous study advisors Kyrre Grøtan and My Hanh Tu for their efforts in structuring my studies.

To my mother and father, Alma and Darko Mitrovic, and the rest of family, thank you for your love and care. You have been there since the first day of my journey. I would not have been here if it wasn't for you. Last but not least, my friends Ahmad Tsjokajev, Imen Belhaj, Jeanne Corrales, Markéta Chlubnová, Vanja Mirosavljevic, you are all irreplaceable, and I am grateful for having you accompany me in this scientific journey of mine.

Abstract

Many neural circuits are perpetually balancing between maintaining existing structure and changing in order to accommodate new information. In this regard, the hippocampus is a brain region known to play a crucial role in both learning and recalling previously acquired knowledge.

The hippocampus has been extensively studied for its role in spatial navigation and episodic memory. The principal neurons of this region are known as place cells. These cells exhibit highly specific spatially modulated activity, and are also known to play a major role in the episodic memory processing.

When introduced to a novel environment, place cells remap, by changing their firing location and/or firing rate. This ability to form orthogonal maps satisfies the need for high-capacity of memory storage. Moreover, some neurons become silent, and other neurons are recruited, providing a different population of place cells coding for different environment.

This master's thesis project investigates how local extracellular stimulation affects spatial tuning in active place cells. The post-stimulation activity in silent cells was also observed. Additionally, this study addresses some limitations of other methods used for direct manipulation of place cells that either lack the ability to observe stimulation effects over a longer period of time (juxtacellular stimulation) or precisely enough targeted stimulation (optogenetics). Furthermore, these methods can be experimentally challenging and very time consuming compared to extracellular stimulation, in which both electrical stimulation and recording of neural activity is performed with a single implantation device. It also allows to track place cell's activity after the stimulation over the course of a few days at least. However, the selectivity of electrical stimulation is not as precise as juxtacellular stimulation, but it is superior to optogenetics.

The results of this study suggest that extracellular stimulation of place fields in well established place cells can induce remapping, much like under natural changes in environmental conditions. Silent cells were also activated with an overall increase in spatial correlation in reference to the stimulus location.

Contents

1. Introduction

> Space is nothing else than the form of all phenomena of the external sense. [...] all phenomena can be given in the mind previous to all actual perceptions, therefore *a priori*, and [...] as a pure intuition, in which all objects must be determined, can contain principles of the relations of these objects prior to all experience
>
> *Kant (1855)*

There are numerous functionally and anatomically distinct areas in the brain, each consisting of billions of neurons with an extremely high number of interconnections, and each system is responsible for a variety of different functions. Among those functions are processes of learning, remembering, and recalling. Learning is the process of acquiring new knowledge or skill and memory is the retention of the information acquired. In particular, remembering is the process of retaining that acquired knowledge, while recalling is a process in which a memory is being retrieved.

Memory is categorized into two main groups: declarative and non-declarative memory. Memory of events (episodic memory) and facts (semantic memory) falls under declarative memory, while memory of habits and skills (also called procedural memory) are considered to be non-declarative types of memory. When new memories are formed, the connections between neurons change. The capability of the brain to change and adapt is referred to as neuroplasticity. The connection between two neurons, referred to as a synapse, is a specialized junction between the axon of one neuron (presynaptic) and dendrites of another neuron (postsynaptic); however, synapses can exist between neurons and muscle cells as well.

1.1 Learning and synaptic plasticity in neural circuits

Neural circuits are perpetually balancing between maintaining existing structure and changing in order to accommodate new information. Both processes are extremely important. Maintaining existing structure without the ability to change it (too little plasticity) renders an organism unable to learn, while changing without maintaining the existing structure (too much plasticity) puts newly acquired information at risk in the long term.

The mechanism of synaptic plasticity was first proposed by Hebb (1949). His hypothesis is that synaptic efficacy is increased when a presynaptic cell stimulates a postsynaptic cell repeatedly and persistently. This type of synaptic plasticity, also referred to as homosynaptic plasticity, is considered to be input-specific as almost simultaneous co-activation of presynaptic and postsynaptic neuron is needed to strengthen the synapse (Markram et al. 1997; Abbott and Nelson 2000; Bittner et al. 2017). Another type of plasticity, known as heterosynaptic plasticity, is a process of weakening or de-potentiating synapses in which the presynaptic activity is absent during a strong postynaptic activity (Lynch et al. 1977; Chistiakova et al. 2014). Both of these forms of plasticity can occur on the same neuron simultaneously (Chen et al. 2013b), supporting synaptic competition (Elliott and Shadbolt 2002; Finelli et al. 2008) as well as preventing synaptic saturation (Wu and Yamaguchi 2006).

The molecular mechanism for long-lasting increases in synaptic strength by principles of Hebbian theory was first described by Bliss and Lømo (1973). This process is termed long-term potentiation (LTP), and it is thought to be essential for episodic long-term memory formation.

1.2 The hippocampal formation (HF) and its role in memory processing

1.2.1 Early studies in humans and other organisms

The hippocampus, also termed as hippocampal formation (HF), is a region found within the medial temporal lobe. One of the earliest studies of the HF in humans was conducted with patient H.M. (Scoville and Milner 1957) who suffered from epilepsy. The treatment for this disease in the case of H.M. was the bilateral removal of the medial temporal lobe extending posteriorly for a distance of 8 cm, which included the hippocampus. After the operation, the patient was showing symptoms of severe anterograde amnesia, but he could still remember episodes from his early life as well as learn new motor skills. Additionally, his short-term memory (lasting seconds to minutes) was intact.

A number of studies, mostly conducted in rodents, were carried out to further investigate the role of the hippocampus in memory. It was proposed by O'keefe and Nadel in 1978 that the hippocampus is a cognitive map. The authors found place-encoding units, later coined as place cells. Their activity depends on the animal's location in the environment. This location where the place cells display the highest firing rate is called place field.

Later, a study was conducted with London taxi drivers to investigate which

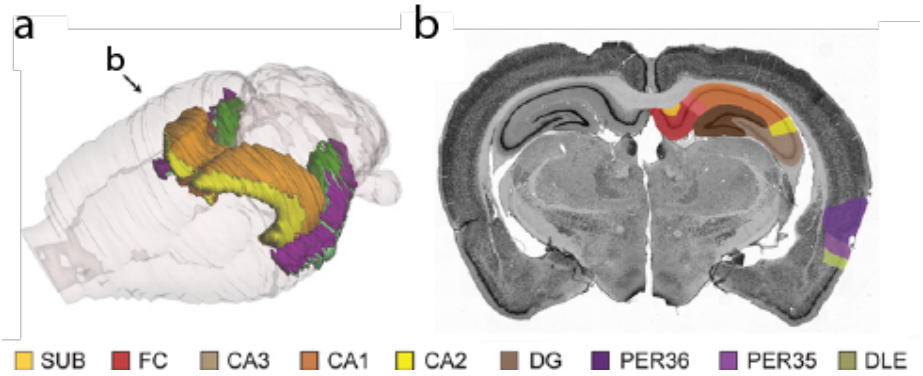

Figure 1.1: The hippocampal region in 3-D and an example of an atlas image from the Rat Hippocampal Atlas a) A 3-D reconstruction showing color-coded surface representations of hippocampal structures (based on the atlas presented in Hjornevik et al. 2007). The arrow indicates the location of section shown in b). **b)** Atlas image of NeuN stained sections with graphical overlay showing color-coded segmentation of the hippocampal region (as presented in the Rat Hippocampal Atlas). Abbreviations: SUB - subiculum, FC - fasciola cinereum, CA - cornu ammonis, DG - dentate gyrus, PER - perirhinal cortex, DLE - dorso-lateral entorhinal area. Adopted from Kjonigsen et al. (2011).

parts of the brain are activated during recall of topographical compared to non-topographical knowledge (Maguire et al. 1997). At the time, retrieval of topographical memory, also called spatial memory, seemed to remain a function of the posterior brain.

1.2.2 Hippocampal anatomy

The HF elongates in a C-shaped manner along the long (septotemporal) axis (Amaral and Witter 1989, Fig. 1.1a). This structure constitutes three different subregions: CA1-3 (from the latin *Cornu Ammonis*, which means the horn of the ancient Egyptian god Amun) subfields of HF, also called the hippocampus proper, the dentate gyrus (DG) and the subiculum (Fig. 1.1).

The HF and parahippocampal region (PHR) together comprise the hippocampal region (Cappaert et al. 2015), which is a part of the old brain (allocortex), and that has been conserved across mammalian species both structurally and functionally (Manns and Eichenbaum 2006). In contrast to HF, PHR includes cortical areas that are reciprocally connected to the HF (Cappaert et al. 2015; Kjonigsen et al. 2015).

The major input from the entorhinal cortex (EC) to the trisynaptic circuit of the HF comes through the perforant pathway (Andersen et al. 1971; Amaral and Witter 1989). The strong projection from EC reaches granule cells in the dentate gyrus (DG) (Andersen et al. 1971). The DG is a C-shaped structure (Fig. 1.1) composed mostly of densely packed granule cells (West et al. 1994; Schultz and Engelhardt 2014). From the granule cell layer, mossy fibres project to the CA3 region of the hippocampus proper, and terminate there (Ribak et al. 1985; Schultz and Engelhardt 2014). CA1 then receives input from CA3

via the Schaffer collaterals, which terminate throughout the stratum radiatum and stratum oriens of CA1 (Ishizuka et al. 1990; Schultz and Engelhardt 2014). Most axonal branches of pyramidal cells coming from CA1 terminate in the subiculum, a structure located between the EC and CA1 (Tamamaki et al. 1987; Amaral and Witter 1989), while some project to the EC, also located in medial temporal lobe (Swanson et al. 1978).

The EC is comprised of medial entorhinal cortex (MEC) and lateral entorhinal cortex (LEC) divisions. Input from spatially tuned cells in the medial entorhinal cortex (MEC) is conveyed to proximal CA1 and then distal subiculum (Tamamaki and Nojyo 1995), while axons from lateral entohinal cortex (LEC) (from cells that are not spatially tuned) convey information to the distal region of CA1 and adjacent proximal region of subiculum (Tamamaki and Nojyo 1995; Witter et al. 2000; Naber et al. 2001).

The CA1 subfield, which is the major hippocampal output, is a feed-forward network, namely, there are nearly no direct interconnections between excitatory pyramidal cells. The CA3 subfield, on the contrary, is wired as a recursive network of pyramidal cells that are densely interconnected and form a recursive circuit (Amaral and Witter 1989).

The CA2 subfield has not been explored as much as the other CA subfields, but it has started to gain popularity over the years. Some key properties that distinguish CA2 neurons from those in CA1 and CA3 were observed (Dudek et al. 2016) including unique gene expression (Lein et al. 2004) and relative resistance to cell death (Sloviter and Damiano 1981; Hatanpaa et al. 2014). Another distinctive property of the CA2 is its connectivity with histaminergic input from the hypothalamic tuberomammillary nucleus (Veazey et al. 1982).

1.3 Spatial navigation in rodents

1.3.1 Discovering place cells

The idea that navigation is guided by internal cognitive maps, first proposed by Tolman (1948), has sparked further research into spatial navigation. Place cells were first discovered by O'Keefe and Dostrovsky (1971). They studied individual neurons in the CA1 subregion of hippocampus in freely moving rats. The main observation was that certain units increased the frequency of action potentials (firing rate) notably when the rat was in a specific location in its environment. These spatially tuned neurons were called place cells. This location in the environment is often referred to as the place field of the putative unit. There was limited evidence for cells with localized firing, but a substantial amount of data was acquired in the following years (O'Keefe 1976).

While place-learning task depends on hippocampus, cue-learning is shown to depend on a different part of the brain during a study where rodents with lesions in fornix (major output tract of the hippocampus) fail to find water during a place-learning task while successfully completing cue-guided task (O'Keefe et al. 1975). In this study, both tasks were conducted on a circular track with 8 water wells placed in the middle of it with equal intervals. In both tasks, the light was illuminating a different well. In the cue-guided task it was illuminating the well with water, while in place-learning task, the light was just a stimulus irrelevant for finding the water. Water was always in the same well in the place-learning

task. Both groups were pre-trained in conditions where wells were filled with water beforehand, but when they consumed all the water, addition amounts were injected if they lick the empty well. During the actual trials, the well was empty. Only in response to licking was the well filled with water.

Ultimately, these findings lead O'keefe and Nadel to believe that place cells are a basic unit of the cognitive map of the animals' environment (O'keefe and Nadel 1978). In addition to this, Morris et al. (1982) showed that lesions in hippocampus cause lasting navigational impairment independent of motor, motivational and reinforcement aspects of the behaviour.

1.3.2 Properties of hippocampal place cells

The spatial information is employed in hippocampal pyramidal cells using rate and temporal codes (Moser et al. 2008). Different place cells have different place fields, while the size of place fields varies along the septotemporal (longitudinal) axis of the hippocampus (Jung et al. 1994; Kjelstrup et al. 2008).

Using ensemble recordings of a fairly small sample of neurons in the hippocampus for collecting information about their joint activity, the animal's exact location can be inferred (Wilson and McNaughton 1993). Another study conducted in the CA3 subfield suggested that these hippocampal place cells send their memory signals to downstream evaluation and decision making modules (Johnson and Redish 2007).

Place cells receive input from mainly two different sources. One input comes from environmental stimuli, and the other conveys information of the internal navigational system that calculates subsequent positions in that environment on the basis of how far (speed cells) and in what direction (head direction cells) the animal had moved (O'Keefe 2014), independently of environmental cues.

Most animals, whether living in water, air, or on land, move in a three-dimensional (3D) environment, yet very little is known on how neural circuits encode navigation in 3D space. However, one study conducted in bats showed that individual neurons in CA1 area indeed encode different 3D place fields (Yartsev and Ulanovsky 2013).

Network dynamics in spatial tuning

Surprisingly, only ∼40% of the spatially tuned principal cells in CA1 are active during behavior, and even less (∼30%) was reported active in CA3 (Karlsson and Frank 2008). The rest of the principal cells, nearly 2/3 are essentially silent during behaviour (reported for the CA1 subfield: Thompson and Best 1989). These silent cells can be manipulated into becoming active via localized stimulus which is described later in this chapter.

Place cells in CA2 are shown to have much more unstable place fields that often change their spatial-firing preference upon novel context which could potentially represent a time-encoding mechanism (Mankin et al. 2015).

Spatial selectivity of place cell in CA1 seems to remain intact after targeted lesion in DG (McNaughton et al. 1989), and after reversible suppression of neural activity in CA3 (Mizumori et al. 1989). Additionally, recursive network appears to be absent in the CA1 in contrast to CA3 (Amaral and Witter 1989). This supports evidence that circuits outside of perforant pathway exist that supply input to CA1 pyramidal cells. Two such functionally distinct circuits

that convey spatial information directly to CA1 are identified. Spatial recall, namely navigational memory, requires input from CA3 to CA1, while recognition memory is sufficiently supported by the input from EC (Brun et al. 2002). Faster manifestation of place cells in CA1 than in CA3 when exposed to a novel environment (Leutgeb et al. 2004) also suggests that CA1 place cells receive direct input from projections from EC which support ensemble of localized firing in CA1 independently of CA3.

Effect of environmental stimuli on place field

Individual place cells are independent of head direction during foraging in a large cylinder (Muller et al. 1994). When rotating controlled environmental cues, however, the place fields rotate accordingly (O'Keefe and Conway 1978; O'Keefe and Speakman 1987). This indicates a direct relationship between the controlled cues and place field. Even after removing the controlling cues, they continue to fire in the previous location. The evidence that the place fields stay the same in relation to lastly seen cues, even after removing the controlled cues, indicates that the place cells possess a sort of "memory".

A similar observation was made in a study with two sets of experiments (Quirk et al. 1990); one where light was initially on and subsequently off and on again (light-darkness-light), and the second experiment where darkness was the initial condition and then the lights were turned on (darkness-light). The same cells were followed in both sets of experiments. In light-darkness-light sequence, most cells retained their place field both during darkness and when the light was turned back on. The same cells did not retain their place fields in darkness-light sequence, but conserved the place field they had in initial darkness condition when the light was subsequently turned back on. These results were to a certain extent in accordance with the previous studies (O'Keefe and Conway 1978; O'Keefe and Speakman 1987).

Most place cells exhibit different firing patterns when changing the environments' shape; the size of place fields scales with the size of the environments, both circular and rectangular settings (Muller and Kubie 1987; O'Keefe and Burgess 1996). Vertical obstacles, both opaque and transparent, that bisect the place field, also attenuate localized firing (Muller and Kubie 1987). This is observed only when exposing the animal to an undistorted environment prior to a distorted one. These studies (O'Keefe and Conway 1978; Muller and Kubie 1987) pinpoint to place fields being linked to external cues, as well as being rotated and scaled according to cues' rotation and environment distortion.

Effect of idiothetic (self-motion) signals on place field

Numerous studies indicate that there is another critical source of place cells' modulation besides environmental stimuli. Most place fields have asymmetric firing fields even though external cues are organized symmetrically (Sharp et al. 1990). In the presence of room cues, distal visual cues predominate over internal cues in establishing place field orientation (Jeffery et al. 1997). A place field size almost never changes with a change in local cue density, spatial frequency or salience (Battaglia et al. 2004). When the rat is rotated independently of the environment, place fields change according to the rat (Jeffery et al. 1997; Jeffery and O'Keefe 1999). Hence, spatial tuning is associated not only with

immediate sensory stimulation, but with idiothetic signals as well.

Head direction cells are cells firing exclusively to a specific head direction in relation to the environment independently of the animal's location (Chen et al. 1994; Taube 2007). They are considered to be a part of path integration system whose metric is self-motion (Taube et al. 1990a; Taube et al. 1990b). It was shown that salient cues stabilize place fields, while in the absence of these environmental cues the place fields start to drift due to accumulation from noise in the motion integration (O'Keefe 1976; McNaughton et al. 1996; Touretzky and Redish 1996; Redish and Touretzky 1997; Samsonovich and McNaughton 1997). However, both place and head direction cells' activity are disrupted when the vestibular system is inactivated (Stackman et al. 2002; Russell et al. 2003).

Virtual environments have allowed conducting experiments such that the vestibular motion input is dissociated from the animal's movement while imaging hippocampal neurons and their activity using calcium indicators (Dombeck et al. 2007; Dombeck et al. 2009; Dombeck et al. 2010). This is typically done by head-fixating rodents that are running on a circular treadmill or a styrofoam ball with visual stimulation of environment on an immersive screen changing according to animal's movement (Dombeck et al. 2007; Dombeck et al. 2010). Hippocampal place cells in the dorsal CA1 subfield exhibit place fields dependent on the distance moved (Chen et al. 2013a; Ravassard et al. 2013), while in the real environment (without head-fixation) they are mostly dependent on absolute position rather than distance moved (Ravassard et al. 2013). When the movement is constricted to two-dimensional virtual environment and with head-fixation, place fields are disrupted (Aghajan et al. 2015), but when the body and head are not in a fixed position, place fields are stable (Aronov and Tank 2014).

Manipulation of different visual cues shows dependence of place fields on a subset of visual cues (Chen et al. 2013a). When all motion is suspended and the animal remains passive during the same visual input from virtual environment, 25% of place cells keep firing locally while the rest (75%) shows changes in firing-pattern (Chen et al. 2013a). When the visual and movement information are conflicting (doubling the speed the animals have to run to achieve the same virtual translation as in the previous trials), the place fields shift backwards, but not to same extent as predicted solely by path integration system (Chen et al. 2013a), meaning that visual information is combined with movement information for computing the place fields. This was demonstrated in freely moving rodents as well (Gothard et al. 1996b; Gothard et al. 1996a; O'Keefe and Burgess 1996).

Global and rate remapping

Manipulation of local and distal environmental cues can induce different changes in place cell's activity, which is referred to as remapping. Leutgeb et al. (2005) demonstrated occurrence of two types of place cells' remapping. When the recording chamber was changed, but its location remained the same, rate remapping occurred, i.e. the place field remained the same and the firing rate varied. On the other hand, changing location of the same recording chamber resulted in global remapping, i.e. change of both location and firing rate making the place field distribution completely uncorrelated. This shows that changes in external cues or even internal factors such as motivation, action plans, etc., lead to rate

remapping, while path-integrator coordinates remain constant.

Further investigation showed that the path-integration system determines whether rate or global remapping occurs (Colgin et al. 2010). This was achieved by introducing a task in which the animals explored chambers of different shapes that are connected, allowing them to move freely between them. Only in this case did the global remapping occur. On the contrary, when the the animals were trained in these two chambers on the same location, it resulted in rate remapping.

This demonstrates an important role of hippocampal neural ensemble in non-spatial as well as spatial episodic memories. The joint nature of spatial and event-based firing is shown through pseudo-random variation in location of different contexts (Komorowski et al. 2009). No significant difference is observed between CA1 and CA3 pyramidal cells.

However, rotating local and distal environmental cues relatively to each other, results in some cells following the local cues while others follow distal cues, and some place cells even become salient, remap or place fields disappear (Tanila et al. 1997; Shapiro et al. 1997; Knierim 2002). These responses are discordant to a greater degree in CA1 than in CA3 (Lee et al. 2004), i.e. most of the place fields of cells in CA1 could not be categorized into one of the responses mentioned above.

1.3.3 Other spatially tuned cells

There is a variety of spatially tuned cells across hippocampus as well as subcortical and cortical regions. All of these cells have increased firing rate according to animal's location, but with different features (Fig. 1.2).

These cells in the EC that are shown to be spatially tuned (Fyhn et al. 2004) are border cells (Solstad et al. 2008), grid cells (Hafting et al. 2005; Barry et al. 2007) and head direction cells that often co-localize with the grid cells (Sargolini et al. 2006).

Boundary cells

There is a population of spatially tuned cells, called boundary cells, that fire most frequently when a boundary is at a particular distance and allocentric direction to the rat (Fig. 1.2b). Boundary cells were computationally modelled (Hartley et al. 2000) and later discovered in MEC (Solstad et al. 2008) and in subiculum (Lever et al. 2009).

Grid cells

Grid cells exhibit spatial firing with place fields organized in a periodic hexagonal manner (Fig. 1.2a) spanning the entire environment available to the animal (Hafting et al. 2005; Barry et al. 2007; Moser et al. 2008; Moser et al. 2017).

The grid cells are described by three characteristics: distance between fields (spacing), angle relative to an external reference axis (orientation), and xy displacement relative to an external reference point (phase) (Moser et al. 2008).

The phase of the grid cells is non-topographic, i.e., it appears to be shifted randomly, just like neighbouring place cells have different place fields, while

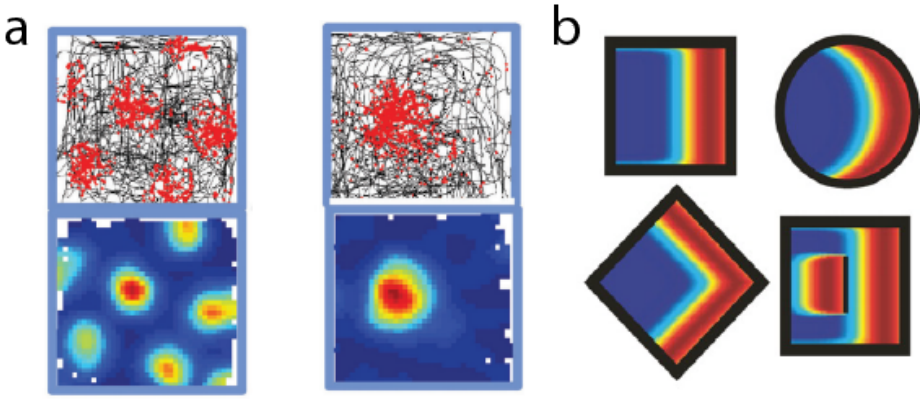

Figure 1.2: Grid cell, place cell and boundary vector cells. a) Grid cell (left) and place cell (right) represented by trajectory map (top) with superimposed spike location (red dots) and rate map (bottom) representing firing rate across the traversed environment (no firing - dark blue, highest firing rate - dark red). Adopted from Moser et al. (2015). **b)** Predicted boundary vector cells rate maps for different environments. Adopted from Lever et al. (2009).

spacing and orientation are topographic. Looking from dorsomedial to ventrolateral MEC, spacing increases (Hafting et al. 2005; Solstad et al. 2007). Orientational topography however, is still not established.

Furthermore, it was suggested that the realignment of grid cells in MEC in association with hippocampal global remapping determines pattern separation, also known as orthogonalization process, in the hippocampal place cells (Fyhn et al. 2007).

1.4 Direct stimulation of place cells

New *in vivo* methods for targeted control of neural activity have been developed over the past years. Bittner et al. 2017 (Bittner et al. 2017) suggested a non-Hebbian plasticity, coined as behavioral time scale synaptic plasticity (BTSP), which underlies formation of place fields in CA1. This is a type of plasticity in which long-lasting plateaus of the membrane potential are more effective in generating global signals that interact with local signals, than brief action potentials. In head-fixed mice running on a linear treadmill, inducing plateau potential initiation in silent cells produced ramp-like depolarization which seemed to drive location-specific firing already in the following lap (Bittner et al. 2017). This ramp-like depolarization was observed to last for several seconds both before and after complex spiking (place fields), hence, having the potentiated input producing predictive place cell activity. BTSP could store a sequence of events in the synaptic weights of area CA1.

One technique that has received a lot of attention is optogenetics, in which a combination of genetic manipulation and optical stimulation makes it possible to target specific cell types for increase or silence their activity (Deisseroth 2011). Boyden et al. (2005) achieved this by introducing a gene for a light-sensitive

cation channel (channelrhodopsin-2) into neurons. The infected neurons would then respond to light stimulation by a depolarisation, leading nearly immediately to action potentials. Later on, a series of other light sensitive proteins have been developed to either excite or inhibit neurons (for review see Deisseroth 2011) and they have been utilized in different ways to study spatial coding in place cells.

For example, the optogenetic hyperpolarization of interneurons (neurons of inhibitory nature) in freely-moving mice, which inhibits activity of inhibitory neurons, leads to reduced spatial selectivity of the place cells suggesting that the role of inhibitory conductance is to suppress out-of-field excitation and limit the dendritic amplification (Grienberger et al. 2017).

Another example with preliminary results shows that optogenetic stimulation of a small group of neurons in freely moving mice, induces place field remapping in CA1 to a greater extent than in CA3 (McKenzie et al. 2019). In addition, the preliminary study observed that novel place fields emerge in both stimulated and non-stimulated neurons. Additionally, other already published studies have found that direct manipulation of local place cell activity (Schoenenberger et al. 2016) can also induce hippocampal remapping.

However, optogenetics does not provide single-cell resolution although it can elicit neural activity in neurons that are at least 50μm apart using μLEDs (Wu et al. 2015). For accurate single-cell stimulation, juxtacellular recording can be used that also allows labeling of the cells for establishment of structure-function relationship (Pinault 1996). Its principle lies in iontophoresis of tracer molecules into the membrane of the neuron through transient micro-electroporation that allows internalization of the tracer molecules (Pinault 2011).

Diamantaki et al. (2018) have managed to record and stimulate pyramidal cells (in CA1 and CA3) in mice while they were running in a circular track using juxtacellular stimulation. They found that the probability of inducing spatial firing in silent cells through juxtacellular stimulation is relatively low ($\sim$32%), while some place cells with already established place fields rapidly remapped ($\sim$45%); otherwise, the cells were not significantly affected by the juxtacellular stimulation. Most of those that did exhibit rapid remapping, remapped to the stimulus location (some also kept firing slightly at the original place field as well). Input-based remapping presented in this study could support rapid formation of orthogonal representations. In addition to this, manipulation of chemogenetic receptors in upstream input from entorhinal cortex (Kanter et al. 2017) have shown to induce hippocampal remapping.

1.5 Aim of study

Studies have shown that place cells are a necessary prerequisite for episodic memory (Smith and Mizumori 2006). Optogenetics and single-cell stimulation, among other methods, have been utilized to examine place cells' plastic abilities and their role in episodic memory; however, long-term effects of these manipulations remain to be investigated. Here, we sought to find answers to this questions through closed-loop extracellular stimulation in the attempt to manipulate targeted place cells and to observe the stimulation effects over longer period of time.

The aim of this study is to extracellularly stimulate a targeted place cell

when the animal is at a position other than the cell's place field, and observe whether the place field of the putative place cell will remap to the new location where it was stimulated; remain unchanged, or perhaps lose its spatial tuning. Additionally, the aim is to observe the duration of these stimulation effects on place units.

Stimulation of targeted place units was accomplished electrophysiologically in a closed-loop manner, i.e. electrical current is automatically sent when set conditions are satisfied during positional readouts, targeting specific place units. The same electrodes are used to measure neural activity. The area of interest was the CA1 subfield of hippocampus proper.

2. Methods

2.1 Approvals

All experiments were approved by the Norwegian Animal Research committee (FDU) prior to initiation. The housing and treatment of the animals are in agreement with European Union and FDU regulations. All researchers involved in the experiments hold an animal researcher certificate that is approved by the Authority for Food and Safety (Mattilsynet). The practical work was carried out in the animal facilities of either the Institute of Basic Medical Sciences (IMB), Faculty of Medicine or the Department of Biosciences (IBV), Faculty of Mathematics and Natural sciences at University of Oslo (UiO).

2.2 Research Animals

Animal model information

A total of 14 male Long Evans rats were used in this study. All animals were between 3-6 months old, and weighed between 300-550 g. Out of these, 6 rats were used for surgical and transcardial perfusion training, another 4 were used for testing coordinates and pilot experiments (#1850, #1824, #1826, #1828). The last 4 were used for the experiments described in this master's thesis (#MBR-0006, #MBR-0007, #MBR-0008, #MBR-0009). One of the experimental rats was terminated early due to complications during surgery (#MBR-0007).

Housing and feeding

Prior to any experiments, the rats were housed in groups of up 3-5 animals per cage, in individually ventilated cages (IVC, GM1800, Scanbur A/S)[1]. All cages were enriched with nesting material[2], Aspen Bricks for gnawing[3], and polycarbonate tunnels[4]. After surgery, the animals were housed separately to minimize the risk of injury to the rat and the implanted microdrives. The rats were kept on a diet of 6-8 food pellets a day in addition to *ad libitum* access to water. The diet is sufficient to maintain bodyweight, but is also sufficient for food deprivation to motivate the animals search for food rewards during

[1] https://www.scanbur.com/products/housing/individually-ventilated-cages-ivc/ventilated-cages-ivc-mice-rats

[2] https://www.scanbur.com/products/consumables/enrichment/paper-cotton-hemp

[3] https://www.scanbur.com/products/consumables/enrichment/soft-hardwood

[4] https://www.scanbur.com/products/consumables/enrichment/polycarbonate

experiments. Temperature and humidity in the IVC cages were monitored and kept constant by the Scanbur system.

The animal facility at IBV follows a 12h light/dark cycle. Because the rats are nocturnal animals, and are active in the dark, all the experiments were conducted in the dark cycle between 12:00 to 00:00. Handling of animals in the cage room during the dark cycle was performed with red lights in order not to disturb the animals.

The experiments lasted for approximately three months, after which the animals were euthanized.

2.3 Tetrode and microdrives assembly

Re-usable standard 16-channel microdrives from Axona Itd[5] were used for measuring electrical activity in the brain. Two microdrives were implanted bilaterally per animal.

2.3.1 Tetrodes

The tetrodes are contructed from a single thread of 17 μm diameter platinum-iridium wire (90% / 10%). The wire was cut to approximately 25cm and taped together in the ends, creating a loop. This was then looped again around a metal arm, and a hook with an attached magnet was hung at the bottom of the two loops. Underneath was a magnet stirrer which, when turned on, twisted the wires into a tetrode. The intertwined wires were fused together using a heat gun for 25 seconds. The tetrode was then cut free, leaving one end with four fused wires and the other end with four free wires. The free wires were briefly exposed to a flame to remove the insulation before assembling them into a microdrive.

2.3.2 Microdrive assemble

The microdrive consist of a connector with 16 attached color-coded cables. The cables are cemented together with a cannula for the tetrodes and a steel frame which makes the tetrodes adjustable (see Fig. 2.2). Four tetrodes are used per microdrive, giving 16 individual electrodes. The fused end of the tetrodes were inserted through the cannula, and each free end of the tetrode was coiled around separate cables of the microdrive. After coiling, each electrode/microdrive connection was secured with conductive silver paint to ensure optimal electrical conductance, and covered with nail polish to protect the wires. The tetrodes are then cut to the appropriate lenght. The final step before implanting is to electroplate the ends of the tetrodes with platinum plating solution to reduce the impedance of each channel (Ferguson et al. 2009) from approximately 1500 kΩ to 100-200 kΩ. On the day of implantation, the microdrives are dipped into 96% ethanol solution for disinfection.

Preparing microdrives for the next use

All the microdrives are reusable, therefore, they need some extra preparation before assembling the tetrodes. The nail polish is carefully removed with ace-

[5] `http://www.axona.com/products/microdrives`

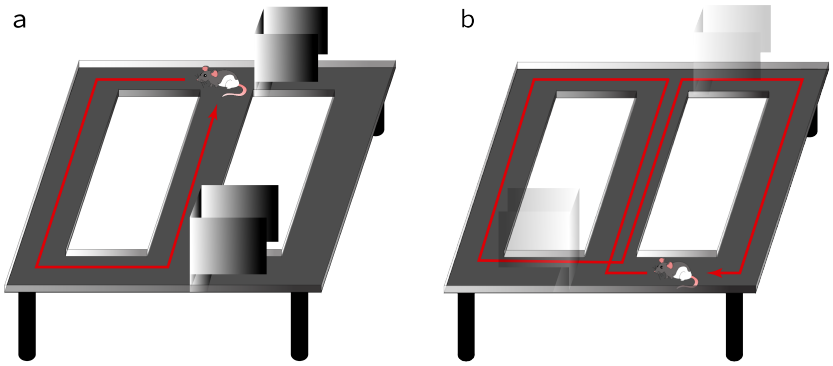

Figure 2.1: Training setup. The eight-track (150 cm length x 150 cm width) with two metal walls (15 cm length x 14 cm width x 25 cm height) as obstacles to direct the rat's movement. The track was surrounded with 2.5 cm high plastic transparent walls. The width of the single track was 14 cm (15 cm including plastic walls). The entire eight-track was surrounded with curtains during experiments (not shown). A camera which recorded animal behaviour was placed above; the field of view covered the entire eight-track (not shown). **a)** The rats were trained to run in the same on one side of the eight-track (150 cm length x 82.5 cm width). **b)** The second experiment was set up such that metal walls were placed diagonally making the rat run in a eight-shaped track. The metal walls were moved concurrently with the rat's movement during the training in order to guide the rat to take alternate turns.

tone in order not to damage the microdrive cables. Then, using a heated scalpel, the cannula is removed by cutting through the dental cement around the cannula. Lastly, a new cannula is cut to a suitable length and cemented onto the microdrive.

2.4 Animal training

In the weeks leading up to the surgery, the animals were handled to get used to humans and also trained for the desired task. If the rats were not comfortable with the experimenter it was more difficult to connect the rat to the recording system and the rat would have poor performance in the trained task. For that reason, the rats were handled on the lap until they were comfortable, with a towel over the lap as they tend to urinate and defecate due to the fear of the unknown.

Rectangular track

In the beginning, the rats were being handled on the lap of the experimenter while given reward treats (Weetos Choco). Once the rats were comfortable being on the lap their training for the task began. The eight-track was limited to a single rectangular track with two metal plates at each cross-section as shown in Figure 2.1. The animal was lured with the treat all the way around until it came back to the same spot, and would receive the treat after each completed

round. After a while, the rat would get a treat after two completed rounds and then three.

Eight-track

The animals were mostly trained on the eight-track. Using the metal plates, they were guided to take the correct turn at the cross. When passing through the central lane, they would alternate between right and left turn every time they came back to the central lane. When the training started, they were lured with the reward to follow the correct path and take correct turns. After a couple of rounds, they would instead receive reward after each correct turn. This training was performed on a daily basis, for 15-20 minutes, for at least a week. After the animals were able to perform the task, the implantation surgeries were performed.

2.5 Surgical procedures

2.5.1 General surgical procedure

Prior to every surgery, all surgical instruments were dry sterilized using a Germinator 500[6] (Braintree Scientific, Inc). The surgery station and stereotaxic frame was wiped with 70% ethanol. All the drugs needed for the surgery were prepared before the animal was anesthetized. The isoflurane (Baxter; Oslo, Norway) was filled as needed. MouseStat System (Kent Scientific, USA) was set up for heart rate and body temperature monitoring during the surgery. The handheld dental drill (W & H Nordic, Sweden), used for performing craniotomies, was oiled before use.

Anesthesia and analgesia

Anesthesia was induced by placing the rat in a small closed chamber filled with 5% isoflurane mixed with pure oxygen. When anaesthetized, the rat was given subcutaneous (SC) injection of Temgesic (buprenophrine, 0.04 mg/kg) for analgesia. For the rest of the surgery the animal was anaesthetized either with 1-3% isoflurane mixed with pure oxygen at a constant flow of 2 L/min, or with an intraperitoneal (IP) injection of Ketalar (ketamine, 0.75 mg/kg) and Domitor (dexmedetomidine, 0.75 mg/kg). In the latter case, Temgesic was not needed. In general, gas anesthesia was preferred over Ketalar injection due to faster post-surgical recovery.

The level of anesthesia was continuously monitored through the MouseStat System and checking the hind paw reflex; anaesthetic dosage was adjusted accordingly.

Head fixation

When the animal was completely anaesthetized, the head was fixed in a stereotaxic frame (World Precision Instruments Ltd, Hertfordshire UK) by placing ear bars in the external auditory canal. The planar line from bregma to lambda was

[6] https://www.braintreesci.com/prodinfo.asp?number=GER

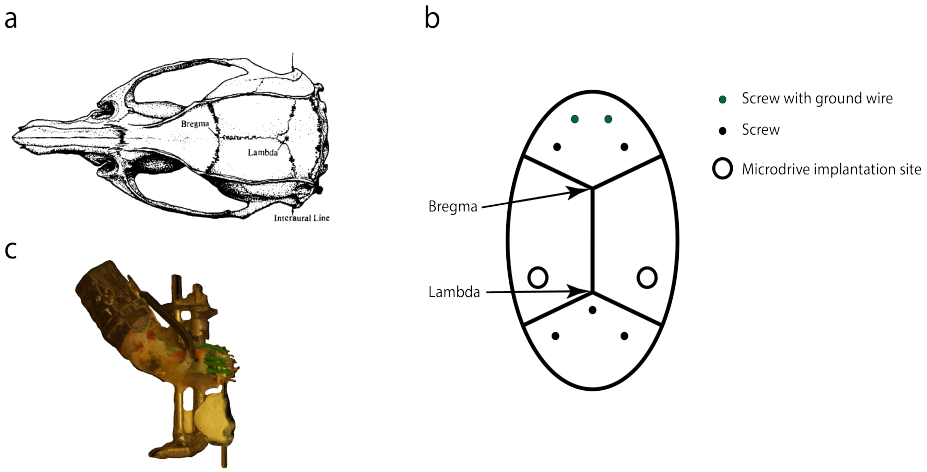

Figure 2.2: Illustrations of implantation position and image of the microdrive. a) Illustration of dorsal view of the skull of a 290g male Wistar rat. Adapted from Paxinos et al. (1985). **b)** Schematic dorsal overview of rat skull with positions of microdrive implantation (empty circles), jewelers' screws (black circles) and jewelers' screws that were connected to the ground wires from microdrive. **c)** Microdrive with mounted cannula, but without any tetrodes inserted.

aligned using the height adjustable nose clamp to ensure correct measurement of implantation coordinates.

The head was shaved from between the eyes down to the neck, followed by disinfection of the area using 70% ethanol, chlorhexidine and iodine solution. For local analgesia, animal received four local SC injections of Marcain adrenalin (bupivacain, 1 mg/kg) around the incision area. A longitudinal incision on the middle of the skull was made from between the eyes down to ears using a scalpel. Using autoclaved q-tips, the blood was removed, and periosteum and skin was moved aside. Artery clamps were used to keep the skin and periosteum away from the craniotomy area. The use of artery clamps was kept at minimum in order to avoid skin wounds. During the entire surgery, 0.9% sterile saline water (NaCl) was applied to prevent the skull and skin from drying out.

Craniotomy

Before performing craniotomies for the microdrives, seven holes were drilled in order to embed jewelers' screws for support and electrical grounding (see fig 2.2.B). The holes were drilled using an automatic drill attached to the stereotaxic frame. The jewelers' screws were stored in 70% ethanol solution before use.

Bregma and lambda were used as skull landmarks for measuring out the correct stereotaxic coordinates for the craniotomies. The craniotomies were then performed using a hand-held dental drill. The stereotaxic coordinates used for the craniotomies were taken from the atlas of the rat brain by Watson and Paxinos (2007).

2.5.2 Implantation of microdrives

Before microdrive insertion, a small incision was made in the dura to allow the tetrodes to be lowered into the tissue. Once the dura was removed, microdrives were mounted onto the stereotaxic frame and the target coordinates were double checked. The following coordinates were used for microdrive insertion in CA1 of the hippocampus: AP: -4 mm posterior to bregma, ML: 3.1 mm, DV: 1.8 mm (AP= anterioposterior, ML= mediolateral, DV= dorsoventral). With the tetrodes resting on the brain surface, the stereotaxic frame was zeroed and the tetrodes were slowly lowered into the tissue. For accurate coordinates of each implantation with necessary adjustments, see 6.5.

After inserting the tetrodes, an outer cannula was lowered from the implant into the craniotomy, and spongostan, soaked in sterile saline water, was used to seal the rest of the craniotomy to protect the tetrodes and the brain from dental cement.

Dental acrylic cement (KA Ramussen, Norway) was applied around the embedded screws, around the outer cannula and to the steel frame of the microdrive to make a firm connection to the skull. The microdrives were detached from the stereotaxic frame once the cement was dry and firm.

The final step was to ground the microdrives. Using a soldering iron, the wires attached to the two foremost jewelers' screws, were soldered to the ground wire on the microdrive.

2.5.3 Post-surgical care

At the end of the surgery, rats were given SC injection of Rimadyl (carprofen, 5 mg/kg) for analgesia. On the skin surrounding the implant, an antibiotic ointment (Fucidin, fucidic acid 2 %) and a pain relieving cream (Xylocain, lidocain 2 %) was applied.

If Ketalar and Domitor were used as anesthesia, the rat received a SC injection of Antisedan (atipamezol, 0.75mg/kg) by the end of surgery for reversal of anesthesia. When isoflurane was used, the animals recovered from anaesthesia a few minutes after being removed from the gas. They were monitored until they started moving again, to make sure everything went well.

For the following three days, Rimadyl was administered once a day together with the Fucidin and Xylocain creams around the implant. If the animals did not eat well after the surgery, they would receive baby food (porridge, HiPP), in order to facilitate their food intake.

2.6 Electrophysiology

For the time constraints, only rectangular-track experiments were conducted and included in the results. A few eight-track recordings were also performed, but not included in this work.

2.6.1 Recording conditions

The experiments were conducted with freely moving rats in the same environment where they were trained (Figure 2.1). The experiments were performed The track was always in the same room at the same spot between each trial

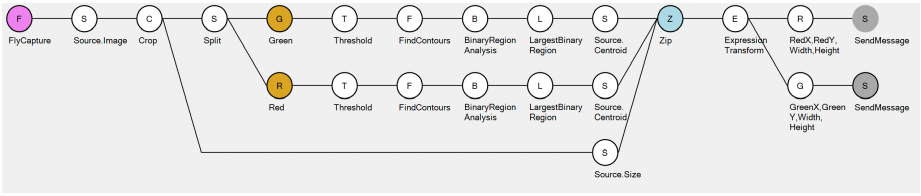

Figure 2.3: Screenshot of Bonsai workflow. The source of frames is chosen (`FlyCapture` and `Source Image`), which is then cropped to only include the track (`Crop`). Green and red LEDs on the headstage are identified using color filters (`Green` and `Red` respectively). The threshold for these filters is adjusted manually (`Threshold`). The x and y positions of each detected LED (`RedX, RedY, Width, Height` and `GreenX, GreenY, Width, Height`) is divided by the width and height of the track, respectively, to normalize the values between 0 and 1. These coordinates are then transmitted to the Open Ephys GUI using Open Sound Control (OSC) protocol (`SendMessage`).

session. In between each trial, the animal was placed back into its cage. In order to prevent different odours from effecting the experiment, the track was washed with soap between each trial session.

When connecting the microdrives the rats were standing still or eating treats. It is important not to exercise too much force onto the implants in order to minimize electrodes' movement. When placed in the track, the cable were counterweighted to prevent them to affect the animals' running behavior.

The room was dark during each trial, which took place during their dark cycle (between 12:00 and 00:00).

2.6.2 Experimental setup

For electrophysiological recordings without stimulation (Fig. 2.4), the Open Ephys (`http://www.open-ephys.org` - Siegle et al. 2017) acquisition board, two Intan headstages RHD2132 with 32 channels (only 16 channels per headstage were recorded) and two Intan SPI cables (1.8 m) were used together with a Windows 10 desktop computer and a USB 3.0 cable for connecting the acquisition Board to the computer. Two custom-made adapters were used to connect the Intan headstages to the Axona microdrives (Fig. 2.4).

Light emitting diodes (LEDs - one red and one green) were mounted on one of the two Intan headstages in order to track the position of the animal during each recording session. A PointGrey Flea3 camera (`http://www.ptgrey.com/`) was mounted on top of the track to monitor animals' movements. The frames were acquired by an open-source software called Bonsai (version: 2.3.1, `https://bonsai-rx.org/`). A Bonsai workflow (Figure 2.3; Buccino et al. 2018) was used to recognize the location of the red and green LEDs. The positions were streamed in real-time to the Open Ephys GUI (version: 0.4.4.1) Tracking plugin (Buccino et al. 2018), for visualization and closed-loop stimulation.

For experiments involving electrical stimulation, the experimental setup required some modifications (Fig. 2.5). The acquisition system was switched to the Intan Stimulation/Recording Controller, that provides the functionality to deliver controlled electrical pulses through the electrodes. Compatible head-

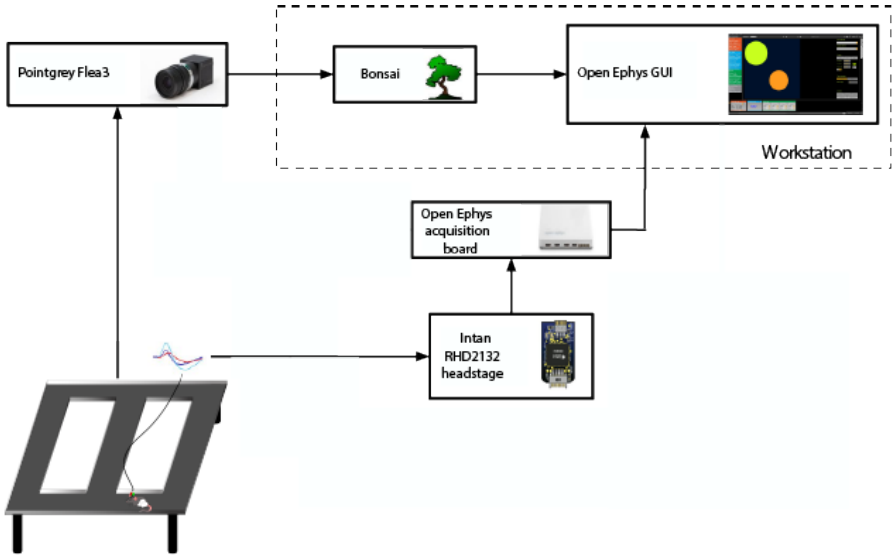

Figure 2.4: Recording setup. Animal's movement in the experimental setup (Fig. 2.1) is captured by the Pointgrey Flea3 camera. The position points are sent to Bonsai GUI, which is further sent to Open Ephys GUI. Electrophysiological data is simultaneously recorded and sent to Open Ephys GUI via Intan headstage and Open Ephys acquisition board. Adopted from Buccino et al. 2018.

stages (32-channel RHS2132 stim/record headstage) and cables (RHS2000 Stim SPI Interface Cables) were used to connect the microdrives to the Intan Stimulation/Recording Controller. The tracking of the animal was performed in a similar matter, using Bonsai and the Open Ephys GUI, the the latter and the Intan acquisition system needed to be synchronized externally. In order to do so, the Pulse Pal 2 stimulator (Sanworks, `https://sanworks.io/`) was used. The Intan Recording/Stimulation GUI (version: 1.05, `http://intantech.com/downloads.html`) was used for acquiring neural rdata and setting stimulation parameters. The electrode channel map was set to match the on used in Open Ephys, to facilitate the monitoring of the recording and the data analysis.

2.6.3 Electrophysiological experiments

Pre-stimulation and post-stimulation trials (recording only)

For each recording, the microdrives were connected to the Open Ephys acquisition board via the Intan SPI cables. Once the microdrives were connected, the LEDs were switched on, and the movement could be tracked.

Before recording of each trial started, rat ID and session number were noted in the control panel of Open Ephys GUI (Figure 2.7). For every 1-2 laps that the rat ran, reward was given manually at a specific location on the track, between

the two curtains surrounding the track. It was dark and quiet during each trial.

A custom-made Open Ephys setup was used to monitor the experiment. the neural recordings were processed online with a band-pass filter for high (300-6000 Hz) and low (<300 Hz) frequency activity, a common median reference node to reduce noise, and a manual online spike sorting method. Different tetrodes were spike sorted separately. The tracking trajectories were visualized in real-time using the Tracking plugin Buccino et al. 2018 (available at `https://github.com/CINPLA/tracking-plugin/`). The tracking timestamps were extracted from the OSC packet received by the Open Ephys GUI.

Each trial lasted for approximately 10 minutes, until the entire track was well covered. After each trial, the data was inspected to identify place cells that could be targeted with electrical stimulation.

Stimulation trials (recording and stimulation)

After a recording session, the data were analyzed as described in Section 2.8.2. Firing rate maps of spike sorted units were visualized and cells with a well-defined place preference (place cells) and a large enough amplitude (>100 μV) were selected for stimulation. For the sake of time, place cells identification was performed visually and without a quantitative analysis on the place field, which

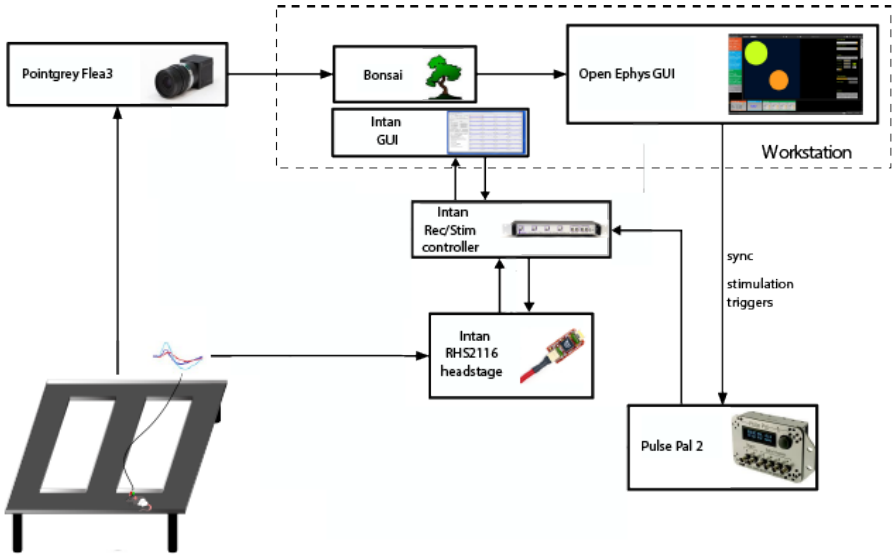

Figure 2.5: Recording-Stimulation setup. Animal's movement in the experimental setup (Fig. 2.1) was captured by the Pointgrey Flea3 camera. The position points were sent to Bonsai GUI, which was further sent to Open Ephys GUI. Electrophysiological data was simultaneously recorded and sent to Intan GUI via Intan headstage and Intan Rec/Stim controller. Pulse Pal 2 is a device used for synchronizing stimulation signals to Intan headstage. Adopted from Buccino et al. 2018.

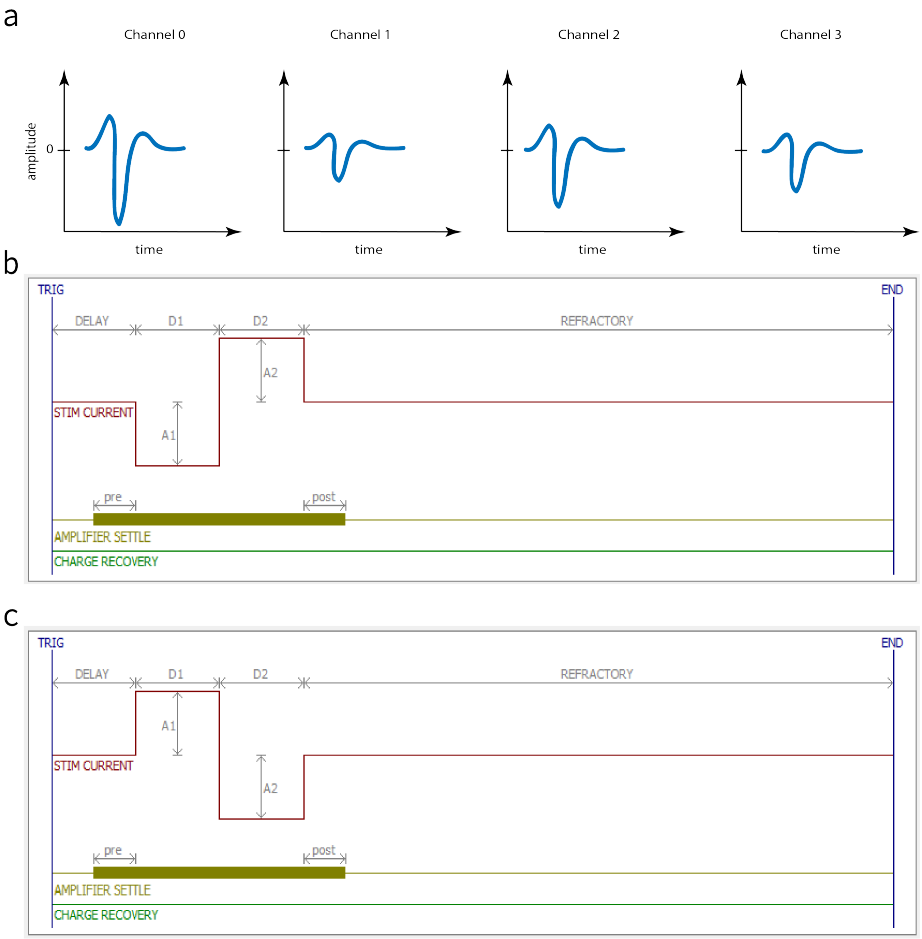

Figure 2.6: Stimulation settings a) Example of waveforms of a target place cell on a tetrode. The channel with the highest amplitude (in this case is channel 0) and the one with second highest (in this case channel 2) are selected for bipolar stimulation. **b)** Biphasic stimulating current for the cathodic-first electrode (sent to the channel with the largest amplitude). Both A1 (cathodic) and A2 (anodic) currents (both phases) had an amplitude of 20 μA. The duration of each phase was 100 μs. **c)** Biphasic stimulating current for the anodic-first electrode (sent to the channel with the second largest amplitude). Amplitudes and phases are the same as in a).

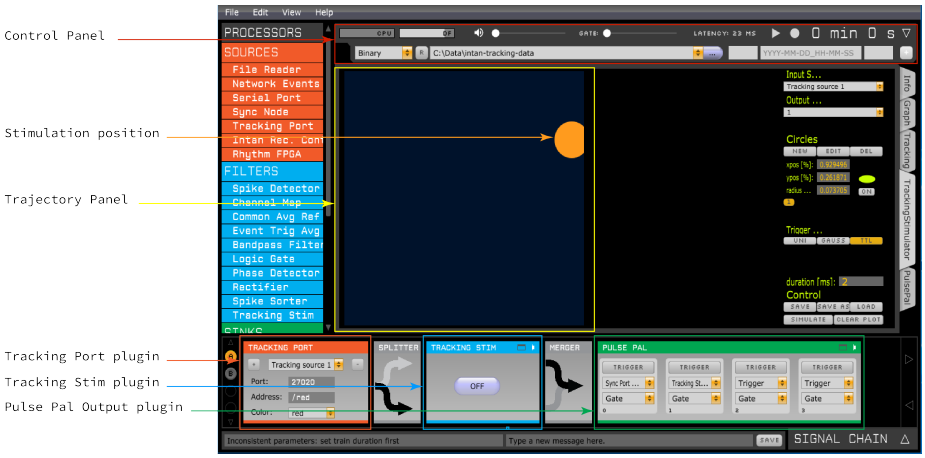

Figure 2.7: Open Ephys GUI. This shows `Tracking Stim` plugin in Open Ephys used in closed-loop stimulation trials. Inside the trajectory panel (yellow) there is a circle that defines at which rat's position the distinct units will be stimulated (light orange). There are three main plugins shown: `Tracking Port` - position data received from Bonsai, `Tracking Stim` - where the stimulation can be turned on or off and `Pulse Pal` - defining outgoing signals (where frequency and length of the signals is defined).

would have required additional time and resources.

After a place cell was identified from each recording, it was followed by stimulation trials.

Stimulation sessions required both the Open Ephys GUI and the Intan GUI in addition to Bonsai. Bonsai and Open Ephys were used for tracking animal's movement and determining when the stimulation signal needed to be sent through Pulse Pal 2. In this case, the Intan GUI was used for recording electrical activity and sending electrical pulses to the electrodes. Stimulation was performed with a biphasic and bipolar paradigm (20 μA, positive and negative phase 100 μs). The cahtodic-first electrode was the one with the largest peak of the mean waveform. The anodic-first electrode was the one with the second largest peak. Stimulation settings in the Intan GUI are shown in Figure 2.6a and b.

The tracking of the animal was performed as described above using the Open Ephys system. Additionally, the *Tracking Stim* node was used to define the target area for stimulation. Whenever the animal entered the target area, a train of 5 trigger events at 20 Hz was sent via the Pulse Pal stimulator to the Intan Recording/Stimulation Controller, that would trigger electrical stimulation of the selected channels. At the beginning of the experiments, the Intan and Open Ephys systems were synchronized by sending a trigger event from the Open Ephys to the Intan system, uing the Pulse Pal stimulator.

The stimulation trials were in general shorter than pre-stimulation and post-stimulation trials. When the trial began, the rat ran 2-3 laps without any stimulation. After that the stimulation was turned on for another three laps aiming for three stimulation periods. Lastly, the stimulation was turned off and the rat ran another 3-4 laps. The whole trial lasted up to 8 minutes.

2.7 Histology

2.7.1 Perfusion and brain sectioning

The termination of rats was done by firstly anaesthetising them in a chamber with 5% isoflurane gas mixed with oxygen. After they were fully anaesthetized, rats received a lethal IP injection of Pentobarbital sodium (50 mg/kg). When there was a complete loss of reflexes, but still a feeble pulse, transcardial perfusion was performed with a phosphate buffered saline (PBS) followed by 4% paraformaldehyde (PFA) in PBS.

The brain was dissected out, and placed in a 25 ml solution of 4% PFA to post-fixate at least overnight. Prior to brain sectioning, it was placed in a 30% sucrose solution for three days to dehydrate the tissue, which prevents formation of ice crystal artefacts in brain sections.

The brain flash-frozen and mounted in a cryostat (CM1950, Leica Biosystems) where it was kept at -19°C while sectioning. The brain was cut into 40 μm thick coronal sections. They were immediately placed onto Polysine slides (Thermo Scientific, USA), and were left to dry for at least 24 hours.

2.7.2 Nissl staining with Cresyl violet

After leaving the slides to dry, they were immersed in Cresyl Violet staining solution for 6-10 minutes, followed by being briefly soaked in Mili-Q water. The process of making the Cresyl violet solution is described in Appendix 6.2. The slides were then dehydrated with increasing concentrations of ethanol. Finally, they were left in Xylene solution for clearing for at least 2 minutes before applying Entellan to secure the cover slip. Excess Entellan on the slides was wiped away with Xylene. Detailed protocol for Nissl staining is shown in Appendix 6.3.

2.7.3 Light microscopy

The sections were photographed at 5x magnification using an AxioCam HRZ camera (Carl Zeiss, Oberkochen, Germany) mounted on an Axioplan 2 microscope (Carl Zeiss, Oberkochen, Germany).

AxioVision software was used for acquiring the images, and the MosaiX module of the software was used to align and stitch the images together. The exposure time was set to 1.8 ms. The distance of the tetrode track was also measured using AxioVision.

2.8 Data analysis

2.8.1 Histology

Section images were inspected and compared to The Rat Brain in Stereotaxic Coordinates (Paxinos and Watson 2007) using a tool developed by Matt Gaidica (http://labs.gaidi.ca/rat-brain-atlas/).

2.8.2 Electrophysiology analysis tools

The data acquired in this project were managed using the Expipe data management system (`https://github.com/CINPLA/expipe`). Expipe enables a tidy organization of recordings and analysis. The data were stored on the NIRD server and accessed through using a *gitea* client. Data were uploaded and downloaded using the GIT Large File System (LFS), in order to maintain version control. The data were stored in *exdir* format (Dragly et al. 2018). In order to perform the analysis, an Anaconda (`https://www.anaconda.com/`) environment was created following the laboratory instructions provided at `https://github.com/CINPLA/expipe`. A custom-made Expipe plugin called *expipe_plugin_cinpla* (`https://github.com/CINPLA/expipe-plugin-cinpla`) was used to register new recordings in the database and perform initial analysis. The plugin provides a graphical user interface (GUI) on Jupyter notebooks (`https://jupyter.org/`) to ease the registration and processing of new datasets.

Spike-sorting

Spike sorting was performed remotely on a lab server using the Kilosort2 (`https://github.com/MouseLand/Kilosort2` - Pachitariu et al. 2016) software within the SpikeInterface framework (Buccino et al. 2019). Before spike sorting, the recordings were bandpass filtered between 300 and 6000 Hz and common median reference was applied to reduce common mode noise. Spike sorting was performed separately for different tetrodes. Additionally, for recordings with stimulation pulses, in order to minimize the effect of stimulation artifacts on spike sorting, a 20 ms period of the signals centered on each stimulation trigger was set to zero.

The spike sorting output was visually inspected and manually curated using the `phy` template GUI. Figure 2.8 shows a screenshot of the GUI, which enables the user to visualize waveforms, auto and cross-correlograms, features, and recording traces. The different plots, or views, were used to clean up the clusters and merge over-split units, following guidelines from the user documentation (`https://phy.readthedocs.io/en/latest/sorting_user_guide/`). In brief, these actions were taken:

- Removal of noisy units: units whose waveform did not resemble an action potential were labeled as noise and removed from the analysis. These units are usually identified when the animal grooms and chews.
- Cleaning of units: the clusters were manually cleanes by removing outliers in the from the `FeatureView`.
- Merging of units: over-split units were manually merged when: i) the mean waveforms had high similarity; ii) the cross-correlograms presented an empty region in the center (due to the refractory period)

After a spike sorting output was curated, the non-noisy units were saved in `exdir` format for further analysis.

2.8.3 Spatial analysis

The analysis was performed using two custom-made Python packages developed by the CINPLA group:

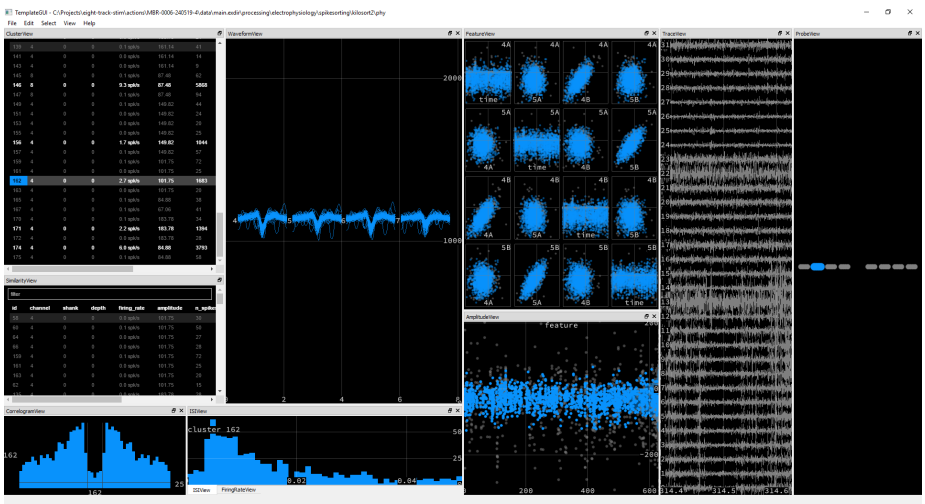

Figure 2.8: Template GUI (phy) showing different features of a single unit after spike-sorting with KiloSort2. It is an interactive visualization of spike-sorted data. `ClusterView` was used for an overview of individual clusters where amplitude and number of spikes were presented. `WaveformView` shows the waveform of spikes on four channels (from single tetrode). Average waveform can also be presented here which was used often when comparing with other units. `FeatureView` was used interactively to remove noise or split clusters. Finally, `CorrelogramView` was used to detect any artifacts that otherwise are difficult to see in other modules. This was used together with `SimilarityView` which shows other units in order of highest to lowest similarity.

- `place-stimulation` (`https://github.com/CINPLA/place-stimulation`)
- `spatial-maps` (`https://github.com/CINPLA/spatial-maps`)

I assisted in the development of the `place-stimulation` repository.

Spike train and tracking information were combined to compute firing maps. The arena was binned using a bin size of 2 cm. The number of spikes per bin (spike map), and the time spent in each bin (occupancy map) were counted. The firing maps were computed by dividing the spike map and the occupancy map, after which they were smoothed using a Gaussian kernel with 3 cm standard deviation (Fyhn et al. 2004). Note that for the stimulation trials, spike trains and tracking needed to be further synchronized using the synchronization trigger recorded by both the Open Ephys and the Intan system.

Sparsity, selectivity and information rate were calculated from the firing maps using `spatial-maps` package. The sparsity measure represents the fraction of the traversed environment in which a cell is active (Skaggs et al. 1996). Selectivity is a measure of how tightly concentrated the cell's activity is. It is defined by maximum firing rate divided by average firing rate (Skaggs et al. 1996). The higher the selectivity value, the more tightly concentrated cell's activity is and cells without any spatial tuning have selectivity value of 1. Information rate, measured in bits/second, is a value of spatial information rate conveyed through the cell's firing rate given the position of the animal. It is based on information theory described by Skaggs et al. (1993). A place cell's information rate would be two bits/second as time and place are the two pieces of information known about cell's activity. However, the background noise is often present in which case the information rate would be a little less than two bits/second.

In order to compare the similarity of firing maps between sessions correlation was used. The correlation between two firing maps was computed by vectorizing the 2D maps into 1D arrays, and by using the `corr` function from the `numpy` package. Bins in the firing maps containing no values (e.g. the center of the map, not covered by the animals) were not included in the calculation.

2.8.4 Statistical analysis

All statistical tests were conducted using `scipy.stats` Python module. For testing whether the spatial correlation had significantly changed after the stimulation for all units found on the channel group through which the stimulation signals were sent, a non-parametric Mann-Whitney U test (`scipy.stats.mannwhitneyu`) was used. For testing whether spatial correlation for only stimulated cells had increased or decreased after the stimulation, non-parametric Wilcoxon signed-rank test (`scipy.stats.wilcoxon`) was used as the two samples (before and after stimulation) are paired. The same test was used for testing changes in other place cell properties such as sparsity, selectivity, average firing rate, etc. These tests were chosen in accordance with finding by Mizuseki and Buzsáki (2013) that the firing properties of hippocampal CA1 place cells are non-Gaussian.

Mean and standard error of the mean were calculated using `pandas` and `numpy` Python packages.

3. Results

Out of 4 experimental rats, closed-loop extracellular stimulation was successfully conducted in 2 rats. The data analysed in the thesis is from these two animals. Only 1 microdrive on each of the 2 rats had recorded units that were used in the data analysis. The focus of the analysis is on the 15 units that were targeted for stimulation.

3.1 Recorded sites in hippocampus

Electrodes were gradually lowered into the dorsal hippocampus CA1 region while the animal was trained in the maze. When place cells appeared, stimulation experiments were started. Recording location of tetrodes at the time of experiment were identified post mortem by light microsope in Nissl stained sections (Fig. 3.1)

The two implants that yielded place units and data used in the analysis both recorded from the CA1 subfield of the dorsal hippocampus proper (Fig. 3.1). This was confirmed after consulting with researches with expertise in this hippocampal area.

Next to CA1 laterally is the CA2 subfield (Fig. 3.1). The wide dense layer of cell bodies is a characteristic of CA2, and both tetrode tracks shown in Fig. 3.1 emerged medially to that layer confirming location of recording to be in CA1.

3.2 The effect of electrical stimulation on place fields

As the animals were trained in the same environment before the experiments, the spatial map was assumed to be well established before the experiments started.

After baseline recording, we chose to stimulate a cell with large amplitude and in a location of the track with minimal activity (Figure example).

The effects of stimulation were quantified by calculating average and maximum firing rate, sparsity, selectivity, information rate in the sessions before and after the stimulation (Fig. 3.2).

Due to stimulation artifacts on the recording trace, we removed 20 ms around each stimulation signal. This might have lead to removal of some spikes as well. For this reason, analysis was mostly focused on the sessions before and after stimulation.

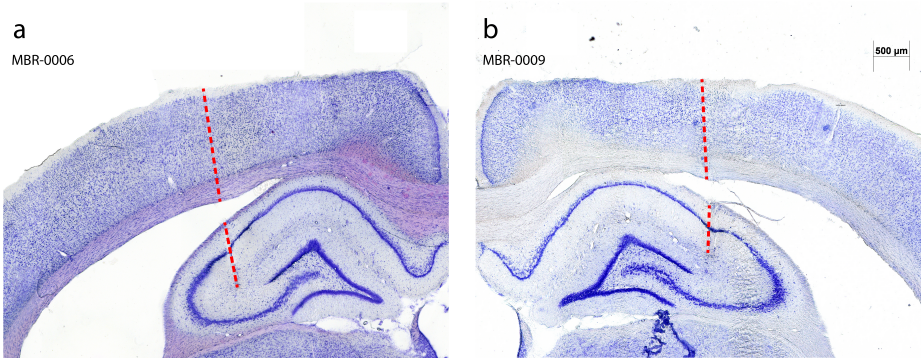

Figure 3.1: Nissl stained coronal brain sections depicting the recording sites. a) Brain section of the left hemisphere of the rat MBR-0006 with marked tetrode track (red dashed lines). These tetrode tracks are within CA1; medially to CA2. **b)** Brain section of the right hemisphere of the rat MBR-0009 with marked tetrode track (red dashed lines). These tetrode tracks are within CA1; medially to CA2. The images were labeled Adobe Photoshop CC.

The one-tailed Wilcoxon signed-rank test showed that there was no significant increase in neither selectivity (p=0.81), nor in information rate (p=0.99) after the stimulation; while no significant decrease was present in sparsity (p=0.99). No significant change was noticed in maximum firing rate (p=0.86), nor in average firing rate (p=0.26).

While the average numbers of the firing activity of the neurons did not change in a specific direction after stimulation, the location of the firing did. Spatial correlation in reference to the original place field (PRE) was significantly decreased (p=0.0003, Wilcoxon signed-rank test); while spatial correlation in reference to the location of stimulation (STIM) was significantly increased after the stimulation (p=0.002, Wilcoxon signed-rank test). This suggest that the place fields have most likely remapped to the location of stimulation (spatial correlation (STIM): PRE n=15, mean ± s.e.m.; -0.06 ± 0.03, STIM n=11, mean ± s.e.m.; 0.08 ± 0.04, POST n=15, mean ± s.e.m.; 0.23 ± 0.07, Fig. 3.2).

The maximum firing rate and spatial correlation in reference to the original place field (PRE) was tested also with two-tailed Wilcoxon signed-rank test for determining whether there was change in these values. The maximum firing rate was not significantly changed (p=0.86), and spatial correlation (PRE) was decreased (p=0.0007), which suggests that place fields in the stimulated place cells have remapped.

These cells were quantitatively categorized into three groups: i) place cells whose place fields remapped to the targeted area, ii) place cells that did not exhibit large changes in firing, and iii) those that started firing diffusely.

Firstly, units that did not exhibit a large change in spatial correlation, sparsity, or selectivity were extracted. The cells that did not show large changes in neither spatial correlation (compared to the targeted area), sparsity nor selectivity (units in shaded region in Fig. 3.3) were selected as those that were unchanged.

Secondly, units that showed increase in spatial correlation to the targeted area after stimulation session and had positive value (red dots in Fig. 3.4c) were

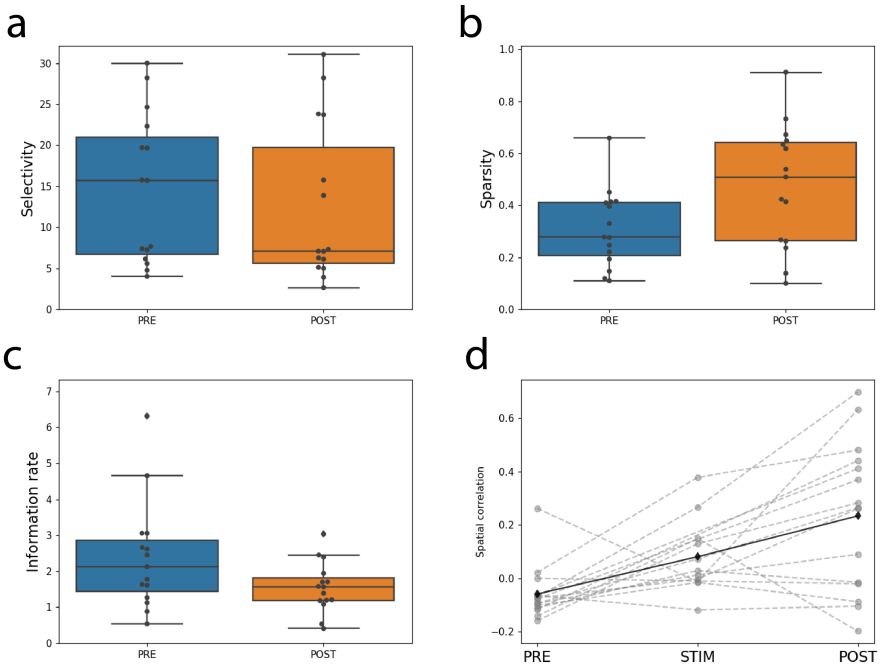

Figure 3.2: Selectivity, sparsity and information rate before and after stimulation session in all analyzed stimulated cells. a) Selectivity comparison between before (n=15, mean ± s.e.m.; 14.6 ± 2.34) and after (n=15, mean ± s.e.m.; 12.5 ± 2.49) stimulation. Stimulation did not lead to a significant increase in selectivity of targeted place cells ($p>0.05$, Wilcoxon signed-rank test). **b)** Sparsity comparison between before (n=15, mean ± s.e.m.; 0.31 ± 0.04) and after (n=15, mean ± s.e.m.; 0.47 ± 0.06) stimulation. No significant decrease in sparsity was present after stimulation ($p>0.05$, Wilcoxon signed-rank test). **c)** Information rate comparison between before (n=15, mean ± s.e.m.; 2.38 ± 0.39) and after (n=15, mean ± s.e.m.; 1.56 ± 0.18) stimulation. No significant increase in information rate was present after the stimulation ($p>0.05$, Wilcoxon signed-rank test). **d)** Spatial correlation for individual units before (n=15, mean ± s.e.m.; -0.06 ± 0.03), during (n=11, mean ± s.e.m.; 0.08 ± 0.04) and after (n=15, mean ± s.e.m.; 0.23 ± 0.07) stimulation in reference to the targeted area. There was a significant increase in the spatial correlation after stimulation ($p<0.05$, Wilcoxon signed-rank test).

extracted and further inspected for value of sparsity to sort them into those that either had remapped or diffused place fields.

Out of these, units that had decrease in sparsity (red dots in Fig. 3.4a) were categorized as the units whose place fields remapped. On the other hand, those that showed increase in sparsity after stimulation session (black dots in Fig. 3.4a) were categorized as units that fired more diffusely. Even though the latter units had increase in spatial correlation for the targeted area, if sparsity was increased, they were likely to fire at both the original location and stimulation location; thus categorized as those with diffused spatial firing.

After sorting the units that had increase in spatial correlation and positive

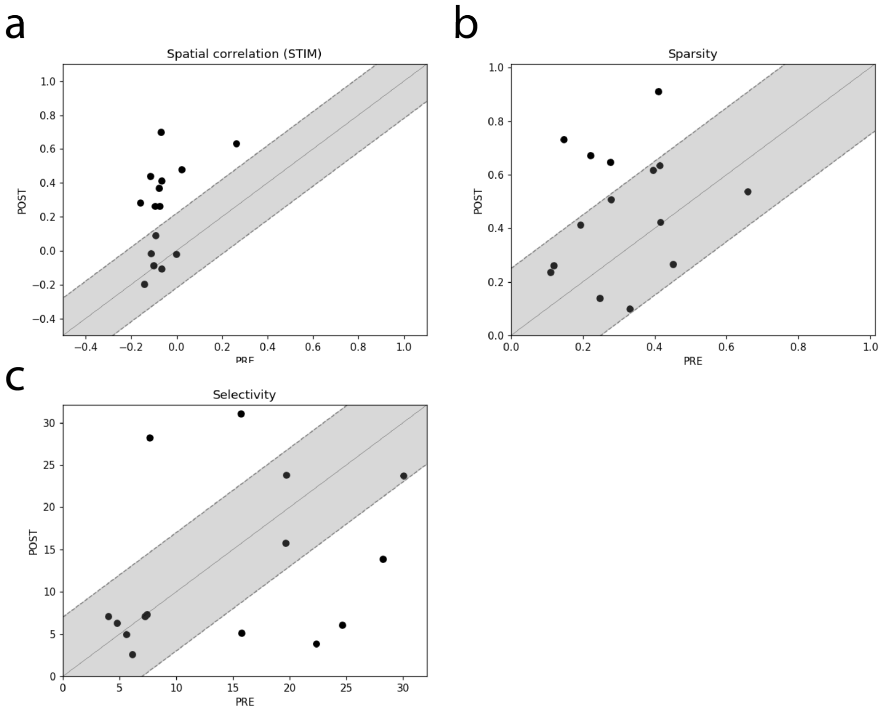

Figure 3.3: Scatter plots of spatial correlation (in reference to stimulation location), sparsity and selectivity from sessions before and after stimulation. a) Scatter plot for spatial correlation of place fields before and after stimulation in reference to the stimulation location. On the diagonal line are all the points for PRE = POST. The units (black dots) that are within the shaded region are those with relatively low change in spatial correlation (POST $\pm$ 0.22 from the PRE = POST line). **b)** Scatter plot for sparsity before and after the stimulation. Within the shaded region are the units with relatively low change in sparsity (POST $\pm$ 0.25). **c)** Scatter plot for selectivity before and after the stimulation. The units withing the shaded region are those that show relatively low change in selectivity after the stimulation (POST $\pm$ 7).

value (red dots in Fig. 3.4c) according to sparsity, selectivity was inspected. Here, the units that had increased selectivity after stimulation session (black dots in Fig. 3.4b) were sorted as those with remapped place fields, while those that had decrease in selectivity (red dots in Fig. 3.4b) were categorized as units with diffused spatial firing even though they had increase in spatial correlation. This could again implicate that the latter units were likely firing at both targeted and original place field location if not over the entire traversed environment.

Finally, the place cells that were left unsorted, were categorized based on average firing rate. Units that exhibited increase in both sparsity (black dots in Fig. 3.4a) and average firing rate (black dots in Fig. 3.5a), and that were not previously categorized were labeled as place cells with diffused spatial firing.

A few place cells disappeared after the stimulation. The data from these units has not been quantified and statistically inspected; however, silent cells appeared to have become active after the stimulation (3.2.4).

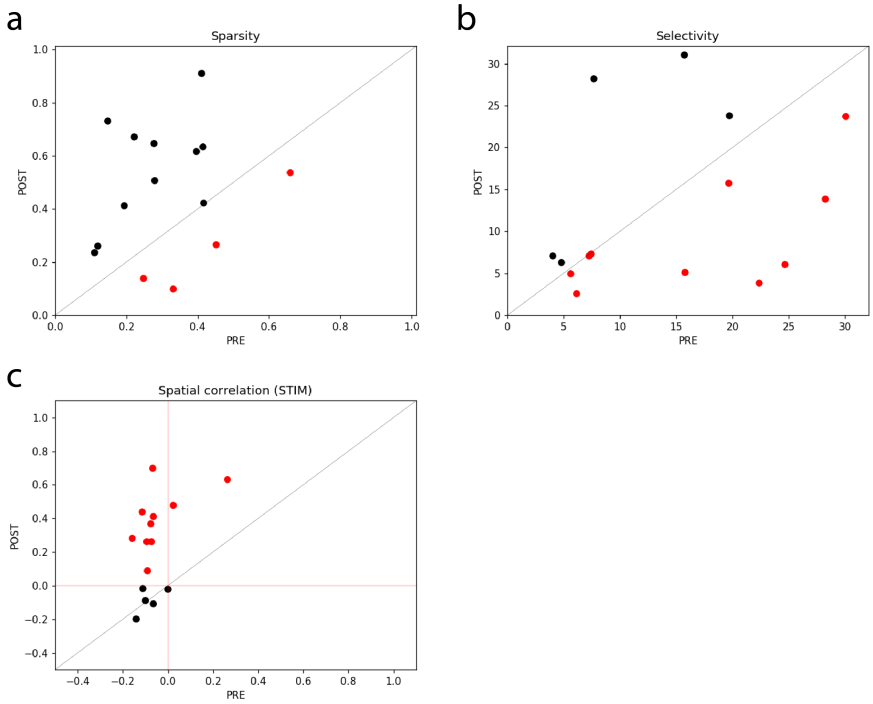

Figure 3.4: Scatter plots of spatial correlation, sparsity and selectivity before and after stimulation. a) Scatter plot for sparsity before and after the stimulation. The units that showed decrease in sparsity (red dots) were used in combination with spatial correlation (STIM) to identify units that have remapped to targeted area. Those with increase in sparsity were most likely units with diffused spatial firing. **b)** Scatter plot for selectivity before and after the stimulation. The units that showed increase in selectivity (black dots) were used in combination with spatial correlation (STIM) to identify units that have remapped to targeted area; otherwise, they were most likely units with diffused spatial firing. **c)** Scatter plot of spatial correlation of place fields before and after the stimulation in reference to the targeted area (STIM). The units that have increase in this spatial correlation after the stimulation and are positive values (red dots) were selected as the units that are most likely to have remapped to targeted area.

3.2.1 Remapped place fields

In Fig. 3.6, an example of a place cell that remapped its place field to targeted location is presented. Increase in spatial correlation to the targeted area (PRE -0.16, POST 0.28), as well as the increase in selectivity (PRE 4.0, POST 7.1) and decrease in sparsity (PRE 0.66, POST 0.54) were measured, indicating that the cell's place field did not only remap, but the cell's activity was more tightly concentrated in the newly formed place field.

There were two place cells categorized as those that changed their place field location to the targeted area (Fig. 3.7) according to spatial correlation, sparsity, selectivity and average firing rate as explained previously.

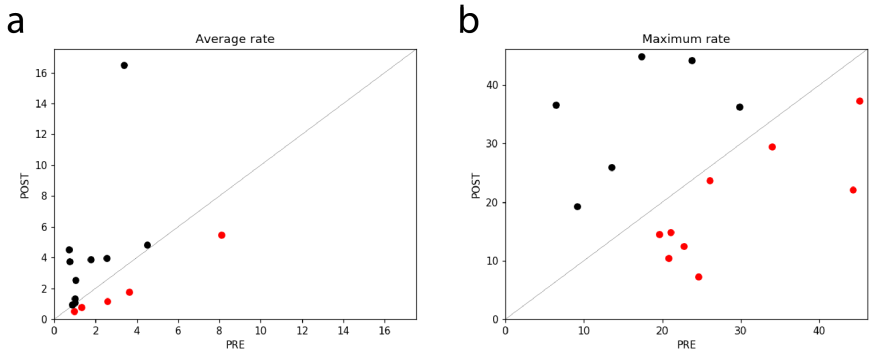

Figure 3.5: Scatter plots for average and maximum firing rate. a) Scatter plot for average firing rate before and after the stimulation. After the units were sorted according to spatial correlation, sparsity and selectivity, the remaining ones were categorized according to average firing rate. Units with increase in average rate (black dots) and increase in sparsity were categorized as those with diffused spatial firing, while those with decrease in average firing rate after the stimulation (red dots) and relatively unchanged sparsity were categorized as units that were unchanged. **b)** Scatter plot for maximum firing rate before and after the stimulation. The units with increased maximum rate after stimulation are marked as black dots, while those with decreased maximum firing rate with red dots.

Statistical test was not conducted in this category since there only are two samples.

Additionally, we observed units that had increase in sparsity after stimulation (3.2.2), although some of them still showed spatial preference for the location of stimulation (Fig. 3.8; Cells 1-5) described later in further detail.

3.2.2 Place cells that exhibited diffused spatial firing

Out of 15 units, 9 cells were quantitatively categorized as place cells that started firing diffusely after stimulation (Fig. 3.8) according to values in sparsity, selectivity and average firing rate as described earlier in this section.

In the example of a cell that had diffused spatial firing (Fig. 3.9), the cell was not detected in the stimulation session. This could be due to a problems in spike sorting due to residual stimulation artifacts. However, the spike-trajectory map as well as rate-map before and after the stimulation are a nice example of a place cell that started to fire more diffusely after the stimulation.

As mentioned in previous subsection (3.2.1), 5 of those cells that lost their spatial tuning still visually exhibited preference for the targeted area or close to it (Fig. 3.8; Cells 1-5). In the whole category, there was a significant increase in spatial correlation in reference to the targeted area ($p=0.004$, Wilcoxon signed-rank test, PRE: $n=9$; mean $\pm$ s.e.m.; -0.04 ± 0.04, POST: $n=9$; mean $\pm$ s.e.m.; 0.36 ± 0.08).

Significant decrease in selectivity was detected in these cells ($p=0.03$, Wilcoxon signed-rank test, PRE: $n=9$; mean $\pm$ s.e.m.; 14.3 ± 2.60, POST: $n=9$, mean $\pm$ s.e.m.; 8.5 ± 2.28); while sparsity was shown to be significantly increased after

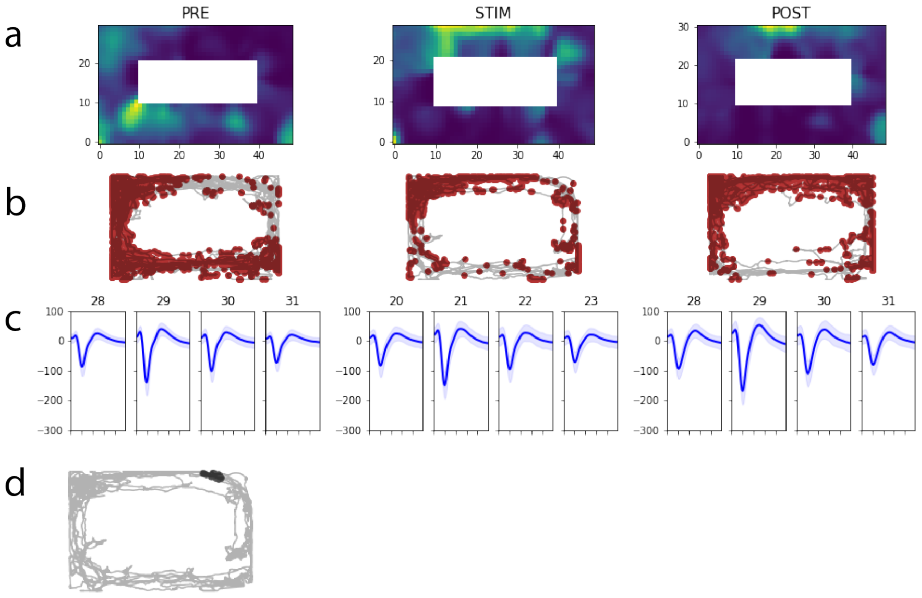

Figure 3.6: Example of stimulation-induced place field remapping a) Rate map: map representing firing rate across traversed environment ranging from no firing (dark blue) to maximum firing rate (bright yellow). Maximum firing rate: PRE 29.8 Hz; STIM 19.2 Hz; POST 36.3 Hz. Selectivity increased after stimulation (PRE 4.0, POST 7.1) and sparsity (the size of the place field) decreased (PRE 0.66, POST 0.54). The place cell fires more tightly concentrated in the remapped place field close to targeted area (d). **b)** Spike-trajectory map: tracked movement of the animal (in grey) with spike location overlaid (red dots). **c)** Single unit waveform on the channel group and corresponding channels (amplitude on channel 29 (absolute value of negative peak of mean waveform): PRE 139 μV; STIM 149 μV; POST 167 μV). The unit was recorded on channel group 7 (right microdrive; rat MBR-0009). **d)** Trajectory map with stimulation signals' (black dots) location overlaid (right)

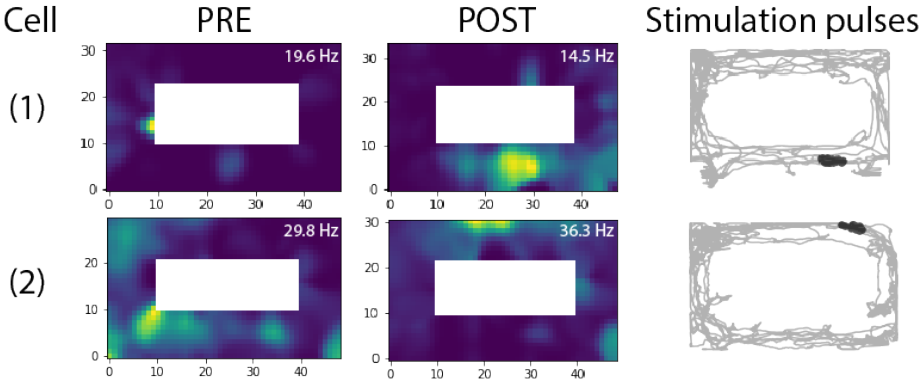

Figure 3.7: Two place cells considered to have remapped after stimulation session. The PRE column shows rate maps of different cells (Cell 1-2) in a session prior to stimulation session. The POST column shows rate maps of different place cells recorded after stimulation that correspond to the cells from pre-stimulation sessions. The last column (stimulation pulses) depicts the location of the animal when the stimulation signals (black dots) were sent. These are the cells that had increased and positive spatial correlation to the targeted area (Cell 1: PRE -0.06; POST 0.41, Cell 2: PRE -0.14; POST 0.28), out which sparsity was decreased (Cell 1: PRE 0.45; POST 0.27, Cell 2: PRE 0.66; POST 0.54). Cell 1 had decreased selectivity (PRE 28.2; POST 13.9), while Cell 2 had increased selectivity (PRE 4.0; POST 7.1) after stimulation.

the stimulation (p=0.004, Wilcoxon signed-rank test, PRE: n=9; mean ± s.e.m.; 0.27 ± 0.04, POST: n=9; mean ± s.e.m.; 0.60 ± 0.06). This is reasonable as sparsity was used for categorization as the main distinguishing feature between the groups.

These units were sorted into this group based on spatial correlation, sparsity, selectivity, and average firing rate; however, this was done without observing specific changes within each pair (PRE and POST). Using Wilcoxon signed-rank test, the same was confirmed for the median difference between individual pairs for individual values. As previously mentioned, more data needs to be acquired to increase the validity of these results.

3.2.3 Place cells that were most likely not affected by the stimulation

Out of 15 stimulated cells, there were 4 cells that were not largely changed in spatial correlation (STIM), sparsity and selectivity (shaded regions in Fig. 3.3), as well as those that had decreased average firing rate among cells with relatively small change in sparsity (shaded region in Fig. 3.3b), shown in Fig. 3.10.

In the example of a place cell that did not visually exhibit place field remapping (Fig. 3.11), increase in selectivity (PRE 15.7, POST 31.1) and decrease in sparsity (PRE 0.25, POST 0.14) is present; similar to the example of place cells that did remap, i.e. the unit is even more selective for and concentrated at the original place field after the stimulation.

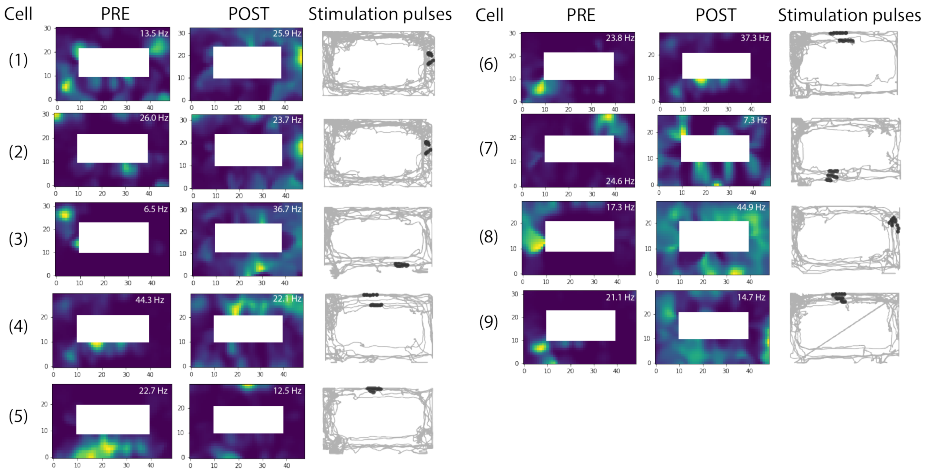

Figure 3.8: All place cells exhibiting diffused spatial firing after stimulation session. The PRE column shows rate maps of different cells (Cell 1-9) in a session prior to stimulation session. The POST column shows rate maps of different place cells recorded after stimulation that correspond to cells from pre-stimulation sessions. The last column (stimulation pulses) depicts the location of the animal when the stimulation signals (black dots) were sent. These cells had significant increase in sparsity after the stimulation ($p<0.05$, Wilcoxon signed-rank test, PRE: n=9; mean ± s.e.m.; 0.27 ± 0.04, POST: n=9; mean ± s.e.m.; 0.60 ± 0.06) as well as increased spatial correlation in reference to the targeted area ($p<0.05$, Wilcoxon signed-rank test: PRE: n=9; mean ± s.e.m.; -0.04 ± 0.04, POST: n=9; mean ± s.e.m.; 0.36 ± 0.08). Selectivity was significantly increased as well after the stimulation $p<0.05$, Wilcoxon signed-rank test, PRE: n=9; mean ± s.e.m.; 14.3 ± 2.60, POST: n=9, mean ± s.e.m.; 8.5 ± 2.28). Cells 1-5 by subjective visual inspection of the rate maps still display preference for the targeted area. The numbers shown on the rate maps is the maximum firing rate.

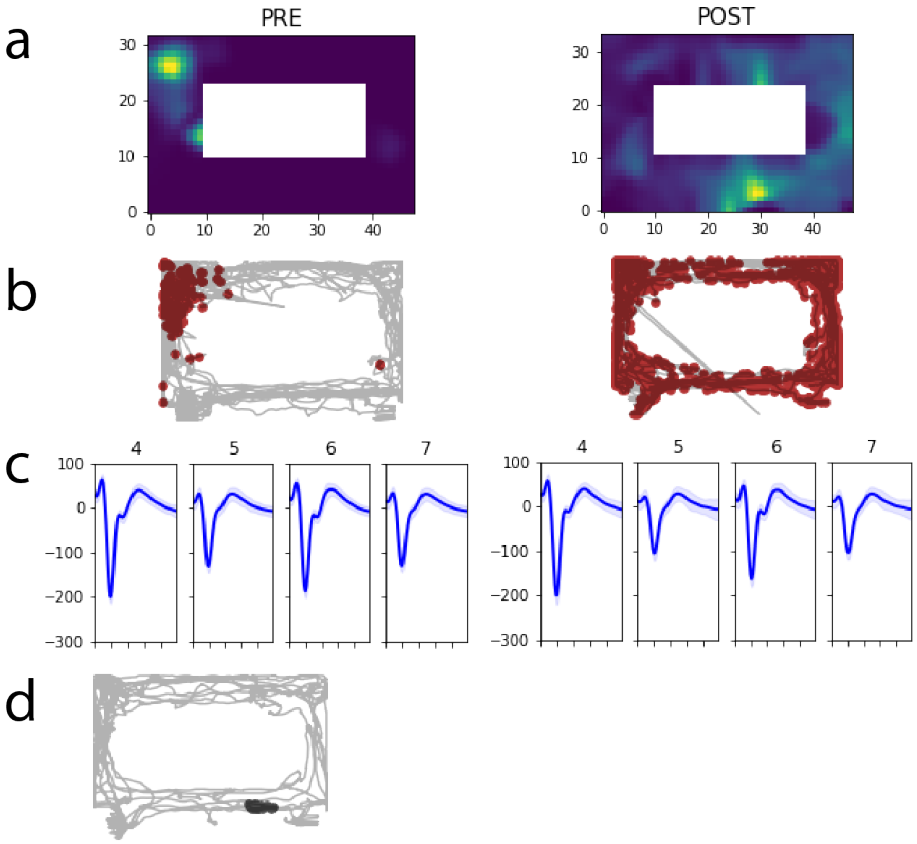

Figure 3.9: Example of a place cell with diffused spatial firing after stimulation session. The unit was recorded on channel group 1 (left microdrive; rat MBR-0006). **a)** Rate map: map representing firing rate across traversed environment ranging from no firing (dark blue) to maximum firing rate (bright yellow). Maximum firing rate: PRE 6.5 Hz; POST 36.7 Hz. Selectivity decreased after stimulation (PRE 7.4, POST 7.3) and sparsity increased (PRE 0.28, POST 0.65) indicating that the cell started firing more diffusely after the stimulation. **b)** Spike-trajectory map: tracked movement of the animal with spike location (red dots). **c)** Single unit waveform on the channel group and corresponding channels (amplitude on channel 4 (absolute value of negative peak of mean waveform): PRE 200 μV; POST 199 μV). **d)** Trajectory map with stimulation signals' (black dots) location overlaid (right)

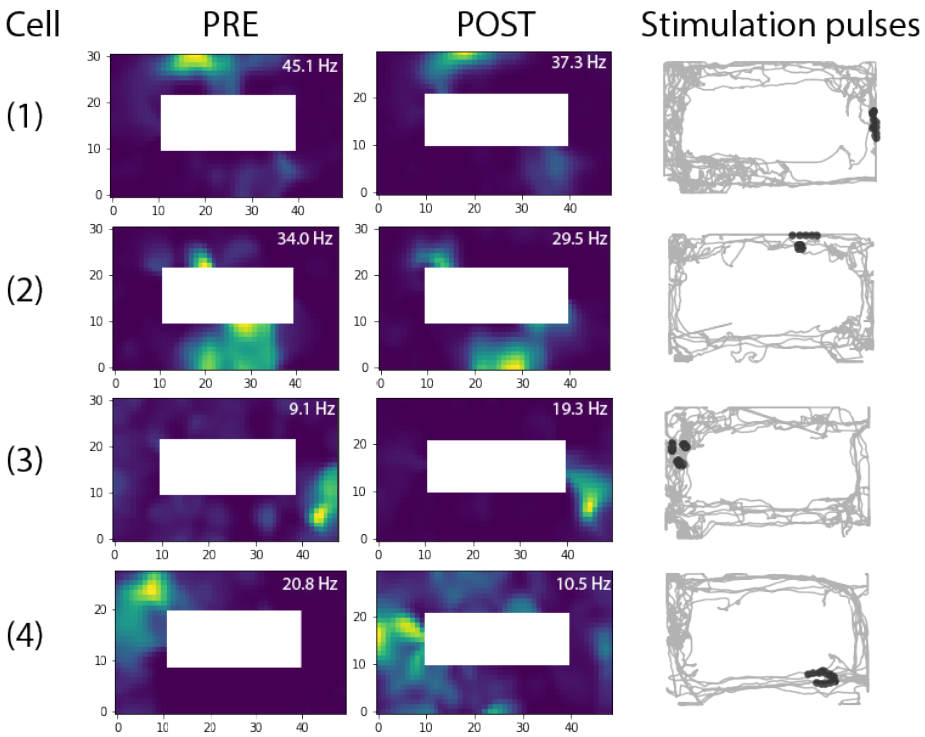

Figure 3.10: All place cells considered not to be largely affected by the stimulation. The PRE column shows rate maps of different cells (Cell 1-4) in a session prior to stimulation session. The POST column shows rate maps of different place cells recorded after stimulation that correspond to cells from pre-stimulation sessions. The last column (Stimulation pulses) depicts the location of the animal when the stimulation signals (black dots) were sent. These place cells' place fields visually seem to not have changed relatively to other cells. There does not appear to be significant change in neither sparsity ($p>0.05$, Wilcoxon signed-rank test) nor in selectivity ($p>0.05$) after the stimulation. The same holds for spatial correlation in regards to targeted area ($p>0.05$, Wilcoxon signed-rank test). The number shown on the rate maps is the maximum firing rate.

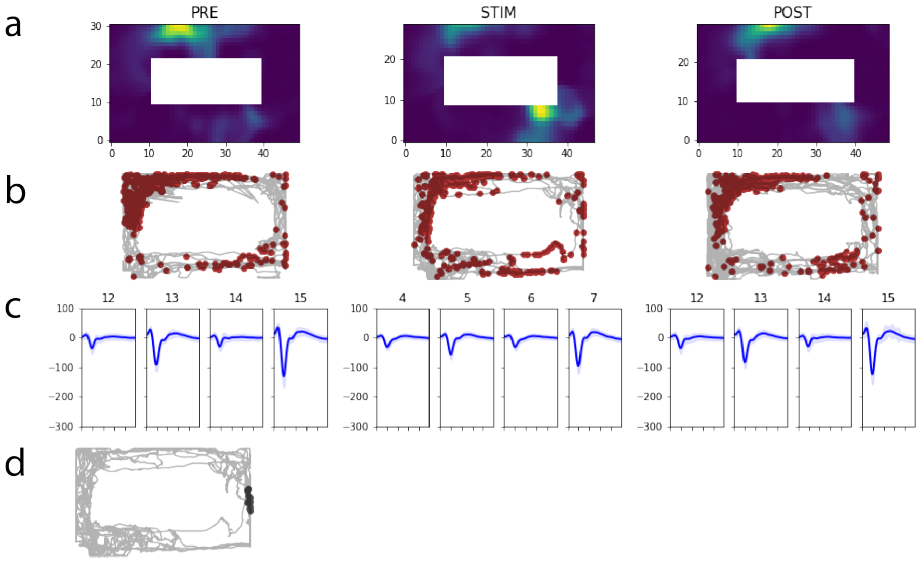

Figure 3.11: Example of a place cell whose place field was not affected relatively to other cells. The unit was recorded on channel group 3 (left microdrive; rat MBR-0006). **a)** Rate map: map representing firing rate across traversed environment ranging from no firing (dark blue) to maximum firing rate (bright yellow). Maximum firing rate: PRE 45.1 Hz; STIM 41.9 Hz; POST 37.3 Hz. Spatial correlation to targeted area: PRE -0.10; POST -0.09, sparsity: PRE 0.25; POST 0.14, and selectivity: PRE 15.7; POST 31.1. **b)** Spike-trajectory map: tracked movement of the animal with spike location (red dots). **c)** Single unit waveform on the channel group and corresponding channels (amplitude on channel (absolute value of negative peak of mean waveform): PRE 131 μV; STIM 94 μV; POST 123 μV). **d)** Trajectory map with stimulation signals' (black dots) location (right)

Overall in this category, there does not seem to be any significant change in neither sparsity (p=0.72, Wilcoxon signed-rank test, PRE: n=4; mean ± s.e.m.; 0.28 ± 0.06, POST: n=4; mean ± s.e.m.; 0.23 ± 0.07), selectivity (p=0.27, Wilcoxon signed-rank test, PRE: n=4; mean ± s.e.m.; 14.5 ± 5.65, POST: n=4; mean ± s.e.m.; 22.3 ± 5.56) nor in spatial correlation in reference to the targeted location (p=1.0, Wilcoxon signed-rank test, PRE: mean ± s.e.m.; -0.08 ± 0.03, POST mean ± s.e.m.; -0.10 ± 0.03) after the stimulation.

As with the previous category with cells that started firing more diffusely after the stimulation, the results of statistical test are in accordance with sorting criteria as expected.

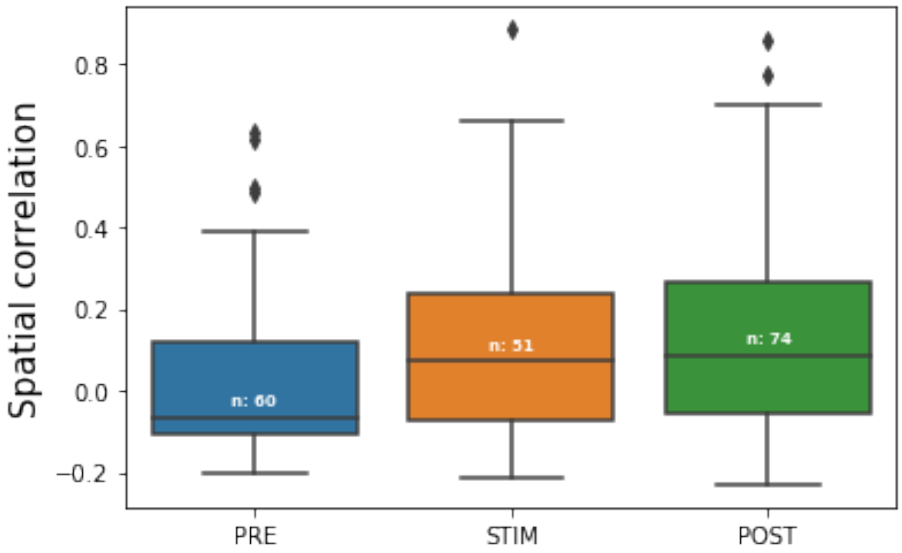

Figure 3.12: Boxplots for spatial correlation of all the units from the tetrode through which the stimulation signal was sent. All the units from the tetrode through which the stimulation signal was sent in sessions before (PRE), during (STIM) and after (POST) the corresponding stimulation session (12 stimulation sessions in total). Applying Mann-Whitney U test, there was a significant change in spatial correlation to targeted area after the stimulation ($p<0.05$).

3.2.4 Silent cells became active

Comparing number of units before and after stimulation on the same tetrode (channel group) where the stimulation signals were sent, there was an increase in number of units recorded after the stimulation (PRE: 60, STIM: 51, POST: 74). The number of units during stimulation, on the other hand, is decreased compared to both before and after stimulation. This is most likely due to removal of stimulation artifacts before spike sorting during during which 20 ms around the stimulation artifact was removed (10 ms before and 10 ms after) as both forward and backward filter passes ware applied. During this process, some of the spikes could have been removed.

There was not only an increase in number of units, but also a significant change in spatial correlation in reference to the targeted area (Fig. 3.12). Mann-Whitney U test was applied to test this ($p=0.004$, PRE: mean ± s.e.m.; 0.02 ± 0.03, POST mean ± s.e.m.; 0.13 ± 0.03).

3.2.5 Effect of stimulation on place cells that were not targeted

In most recordings there was more than one place cell per tetrode in a single recording. Those place cells that were not targeted for stimulation could still be affected by it.

One such example was found that is included in the results (Fig. 3.8 Cell 2).

Increase in sparsity suggests a more diffused spatial firing (spatial correlation (STIM): PRE -0.07; POST 0.70, sparsity: PRE 0.28; POST 0.51, selectivity: PRE 5.56; POST 4.99, information rate: PRE 6.3 POST 3.0).

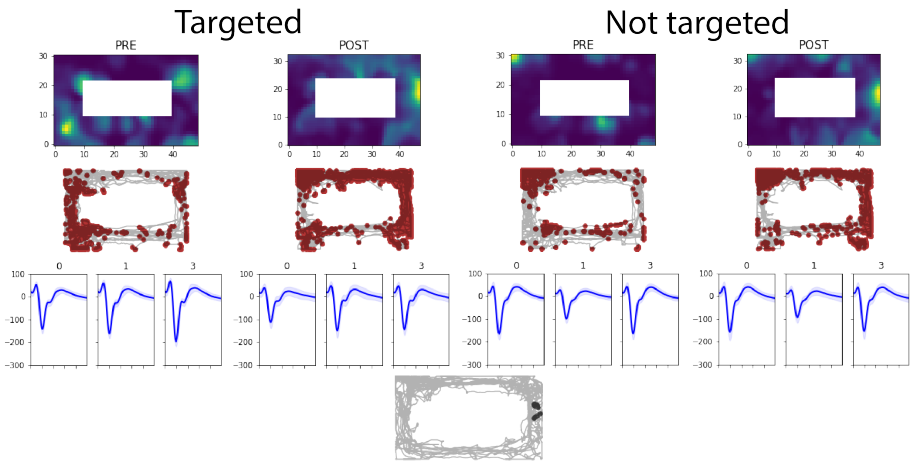

Figure 3.13: Two units on the same channel group where the stimulation signal was sent. Rate map (first row), spike-trajectory map (second row) and single unit waveform (third row) of the unit that was targeted (left) and the unit that was recorded on the same channel group (tetrode), but was not targeted by stimulation (right). The unit on the left was targeted by sending biphasic electric current to the two electrodes where the highest amplitude was recorded; channel 3 and 1 in descending order. The two channels with the highest amplitude for the unit that was not targeted were 0 and 3 in descending order. The unit that was not targeted did exhibit a change spatial firing: spatial correlation (STIM): PRE -0.07; POST 0.70, sparsity: PRE 0.28; POST 0.51, selectivity: PRE 5.56; POST 4.99, information rate: PRE 6.3 POST 3.0. The location of the animal during stimulation signals is shown in the bottom image.

3.3 Duration of the stimulation effect

A previous study (Bittner et al. 2017) performed whole-cell patch-clamp recordings on silent place cells and found similar results with ours; however, it is problematic to record from the same cells over an extended period of time using whole-cell patch-clamping. Nonetheless, we were able to observe long-term effect of the stimulation on remapping with the extracellular recordings over a few days.

Several examples of different long-term effects of stimulation are presented. There is an example of a place cell that remapped to target area after a single stimulation session, and retained its place field there for almost two days (Fig. 3.14).

Several stimulation sessions were conducted targeting single place cell (Fig. 3.15). The first stimulation session (STIM1) did not seem to have an effect on cell's place field. Remapping was observed first after the second stimulation

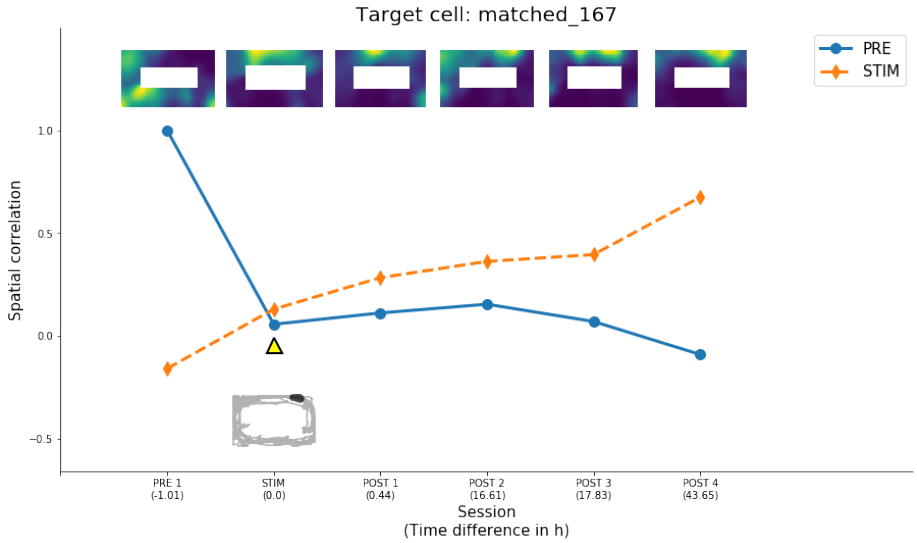

Figure 3.14: Long-term effect of electrical stimulation on a single place cell after one stimulation session. Rate maps (top) of a single place unit (matched_167) before stimulation (PRE 1), during stimulation (STIM) and after stimulation (POST 1-3). Spatial correlation in relation to the initial place field (PRE) is decreased after the stimulation (yellow triangle), indicating that it nearly completely ceases to fire in the original place field. Spatial correlation in relation to targeted area (STIM) is increasing, indicating that the place field is shifting to the targeted area.

session (Fig. 3.15; STIM2), while after third one, the hippocampal place cell started firing more diffusely (Fig. 3.15).

A place cell was observed to start firing at both the original place field and the targeted location during the stimulation (Fig. 3.16; STIM). The effect of the stimulation was followed up in three recording sessions over 24 hours (Fig. 3.16; POST1-3). It was observed that the place field remained at the original location.

There is another example of a cell that exhibited diffused spatial firing after stimulation (Fig. 3.17; POST1); however, the place field returned to the original location (Fig. 3.17; POST2-3).

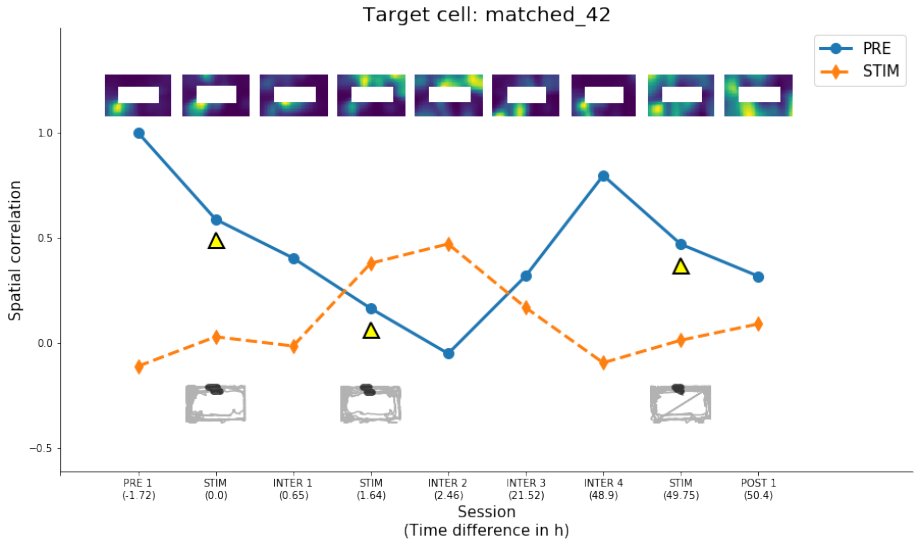

Figure 3.15: Long-term effect on a single place cell recorded after multiple stimulation sessions. Rate maps (top) of a single place unit (matched_42) before, during and after multiple stimulation sessions (marked with yellow triangle). Spatial correlation in relation to the original place field (PRE) is descending after 1st stimulation (INTER1), and significantly more after 2nd stimulation (INTER2); while it increases in relation to the targeted area (STIM). Increase in PRE spatial correlation is observed again (INTER3) as it retains its original place field (STIM). It continues to increase and decrease respectively (INTER4). After 3rd stimulation, the place cell starts to exhibit diffused spatial firing.

3.4 Summary of stimulation effects

Different outcomes were observed in the stimulated units (Fig. 3.18). Overall, there was a significant increase in spatial correlation in reference to the targeted area; and decrease in spatial correlation in reference to the original place field; however, there were units that did not seem to be affected by it (n=4).

In summary, our result shows that targeted electrical stimulation of place cells in area CA1 of hippocampus can induce remapping in a subpopulation of the recorded units (partial remapping).

Even though there were not enough place units to draw any strong conclusions about the closed-loop stimulation effects, the result is consistent with recent studies that utilized different methods (Bittner et al. 2017; Diamantaki et al. 2018; McKenzie et al. 2019).

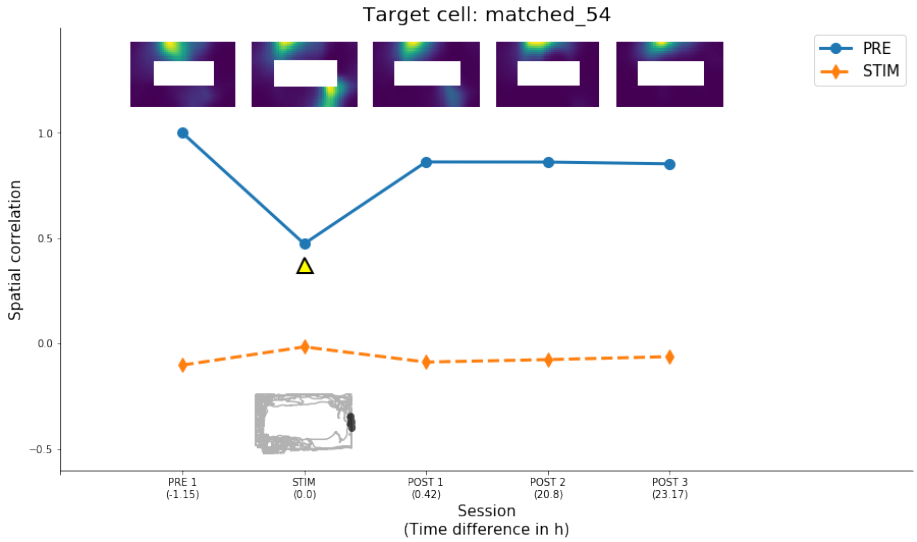

Figure 3.16: Example of an unchanged cell followed up over extended period of time after single stimulation session. Rate maps (top) of a single place unit (matched_54) before, during and after a single stimulation session (marked with yellow triangle). Presented unit was stimulated once (STIM) and recorded over 24 hours after stimulation (POST1-3). There does not seem to be significant change in spatial correlation in reference to the targeted area; while spatial correlation in relation to the original place field (PRE) decreased during stimulation session and increased again afterwards (POST1-3).

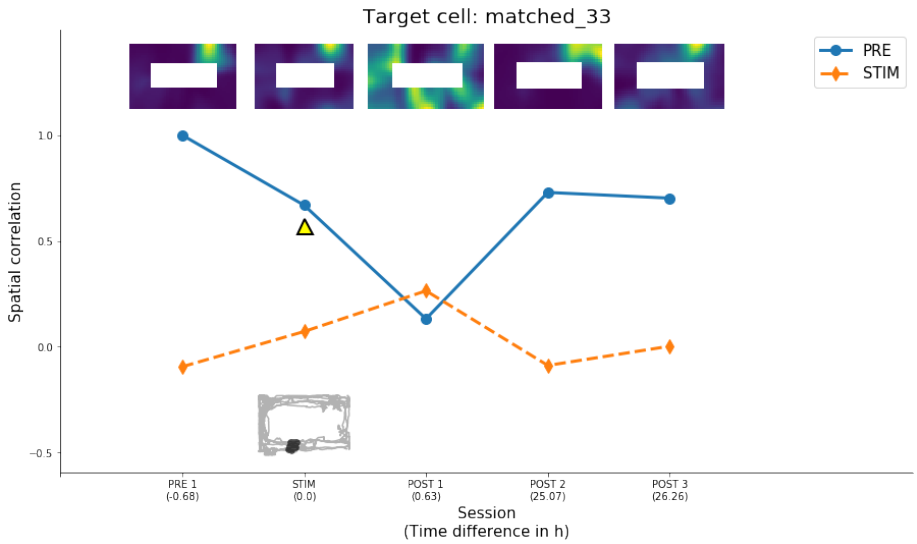

Figure 3.17: Example of a cell with changing firing patterns followed up over extended period of time after single stimulation session. Rate maps (top) of a single place unit (matched_33) before, during and after a single stimulation session (marked with yellow triangle). Presented unit was stimulated once and followed up over 24 hours after stimulation (POST1-3). In the recording session following stimulation session (POST1), both spatial correlations changed (PRE decreased and STIM increased) which resulted in more diffused spatial firing. In POST2-3, the place cell's place field remapped back to its original place field nearly completely.

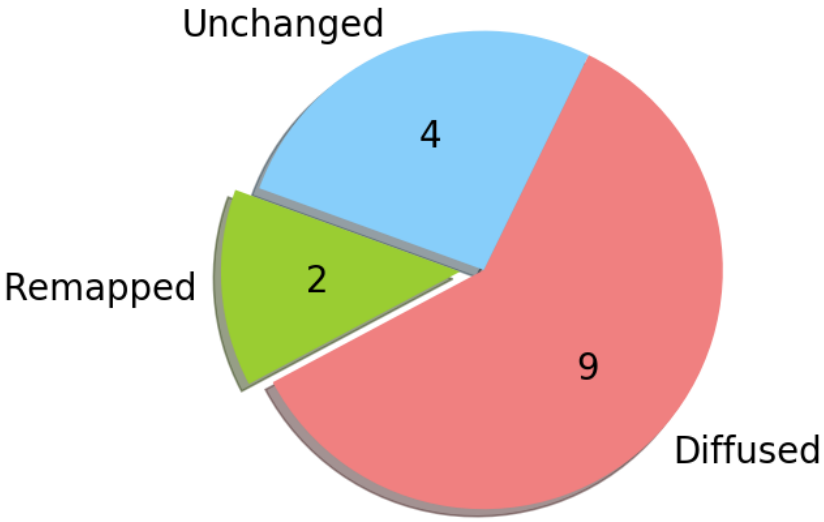

Figure 3.18: Summary of the stimulation effect. Most of the place cells were effected by the extracellular stimulation (n=11); while some did not exhibited significant change based spatial correlation, sparsity and selectivity (n=4). There were only 15 units included in the data analysis, and the purpose of this chart is to simply provide an overview of the results.

4. Discussion

4.1 Main findings

This thesis reports the effects of closed-loop extracellular stimulation in adult Long Evans rats during one-directional movement in a familiar environment. We demonstrate that local extracellular stimulation to a pair of neighboring electrodes could successfully change the localized firing of hippocampal cells. We show that remapping can be induced in individual cells or even in a sub-population of place cells by extracellular stimulation much like under natural conditions, which is in accordance with the previous studies (Bittner et al. 2017; Diamantaki et al. 2018). This was possible even under the conditions in which the hippocampal map is considered to be most stable, i.e., when the rat is in a familiar environment. The spatial correlation in reference to the targeted area was significantly increased after extracellular stimulation in the majority of stimulated cells that we analysed. Nonetheless, there were 4 out of 15 analysed place cells that were quantitatively identified as units without significant change in firing location. Whether the stimulation induced partial or global remapping remains to be elucidated.

The stimulated place cells were observed in multiple cases for over 1-2 days, indicating that the stimulation current did not induce cell death, and the cells remained active.

An increased number of active cells was observed in recording following stimulation session in which significant increase in spatial correlation in relation to stimulation location was present.

4.2 Methodological considerations

Collecting data from a population of place cells involves many time-consuming steps such as animal training, implantation, electrophysiological recordings and analysis; however, the process has been optimizing over the past years and continues to do so. The key was to find balance between efficiency and resources available for the project.

4.2.1 Surgery and microdrive implantation

The coordinates for the implantation are based on locating bregma and lambda correctly. It is additionally dependant on fixing the animals' head properly in the stereotaxic frame in regards to mediolateral and longitudinal axis. This process is prone to human error which could lead to implantation at an area

other than the one initially planned. In addition, large blood vessels such as dural venous sinuses detected in the craniotomy needed to be avoided; hence some adjustments needed to be made whenever that happened. Thus, after the experiments were finished, we verified the location of the recording tracks by histology. The area of interest was still successfully targeted in experimental animals with 5 of 6 microdrives (Fig. 3.1).

Craniotomies were made with great caution, primarily avoiding damage to the cortex or bursting large blood vessels. Nonetheless, slight damages from drilling is generally not considered to impact the place cells' activity. Supporting arguments were made by Dombeck et al. (2010), who actually removed the cortex above dorsal hippocampus (2.77 mm in diameter) for two-photon imaging of place cells in CA1, claiming that it did not affect the results significantly. Compared to such lesions, our lesions are negligible, but there is always a potential for unknown side effects from invasive procedures. These lesions can always be reduced to an extent by slowly advancing the electrodes through brain parenchyma.

Gliosis, a response to damage in the central nervous system by recruitment of glial cells (Pekny and Nilsson 2005), can be caused by lesion made with electrodes advancing through the tissue. This can in turn cause artifacts in the recordings if the electrodes stay for too long in one place, or are advanced through the brain parenchyma too fast.

However, the lesions can be used to our advantage for post-mortem analysis of the anatomical location of recorded place cells.

4.2.2 *In vivo* electrophysiology

Tracking neuronal activity in real time while tracking animal's position is necessary for monitoring place cells. For the purpose of this thesis project, it is advantageous if the animal is allowed to move freely in the environment for observing place cell activity with the least number of behavioural restrictions. The free movement is accomplished with the microdrives and cables that are counter weighted for avoiding any disturbances from the weight of cables and microdrives on animals' heads.

For chronic electrophysiology, two microdrives per animal were used in this thesis project, each equipped with 16 channels (32 channels per animal). An increase in number of electrodes increases the chance of finding place cells; hence less animals are required. This type of experiments started with single electrodes (Zalutsky and Nicoll 1990), moving to movable bundles of 10 electrodes (Thompson and Best 1989), and today there are advanced multi-channel drives such as flexDrive (Voigts et al. 2013) for mice that can carry 64 electrodes per drive, and even Neuropixels probes, with 384 simultaneously recorded channels (Jun et al. 2017b). In order to increase the number of recorded units per animal, future experiments could benefit from using these kinds of recording devices. Nichrome (any of various alloys of nickel, chromium and often iron) was used to make the electrodes in early studies (Thompson and Best 1989), although it can corrode inside the body (Cowley et al. 2011), which makes platinum-iridum wire used in this project the better choice.

Electrode wires of different diameters were tested and the ones that are 17 μm in diameter were proven the most optimal for balancing between impedance and the degree of localization of electrical activity. Impedance can still be

optimized by plating the tips of the electrodes. For electrical stimulation, the target impedance is preferred to be slightly lower than usual ($\approx 100\Omega$) in order to be able to provide the stimulation currents without saturaiton.

Compared to juxtacellular stimulation, which is quite delicate (for detailed procedure in rats see Tang et al.; adjusted for mice see Diamantaki et al.) and very few neurons can be electrophysiologically monitored (Tang et al. 2014), extracellular recordings are a better choice for this project because they enable monitoring of multiple cells simultaneously, and are easier to perform. The current used was quite weak. Additionally, the current was bipolar making it even more selective. It is bipolar because the current that is injected down toward the cells is drawn back up through a different electrode, preventing it from spreading further away from the electrodes.

The stimulation signals conducted through the electrodes recording multiple neurons concomitantly still did effect more than just the targeted neuron as presented in Fig. 3.13. This shows that the stimulation is less selective than desired; however, the amount of current could be slighlty decreased.

4.2.3 Histology

In the beginning, there were problems with brain sections falling off the microscope slides even after treatment with chloroform:ethanol (1:1) solution to dehydrate them before starting the Nissl staining. The problem was solved by either applying poly-lysine solution onto Superfrost Ultra Plus (Thermo Scientific, Hungary) microscope slides and then briefly washing it off, or simply by using Polysine slides (Thermo Scientific, USA) that are already coated with poly-lysine.

4.2.4 Animals' behaviour

Training, feeding schedule, experiments and housing were made as similar as possible for each animal. Each animal is, nonetheless, different and exhibits different behaviour, which could have an effect on the task performance; thereby possibly affecting the results. Increasing a number of animals from which the data is acquired is a solution for avoiding any bias regarding animals' performance.

It was shown that trained attention to certain environmental cues can affect place cell correlates (Zinyuk et al. 2000); even more so than motivation (Kentros et al. 2004); albeit attention and motivation can seem inseparable.

In the beginning of training, animals received reward at random locations on the track to avoid its motivational effect on place field formation (Ólafsdóttir et al. 2015). During experiments the reward was given mostly at single location where the two curtains enclosing the track meet, which according to Kentros et al. (2004) should not affect the stability of already formed place fields.

The animals were trained to move in the same direction. However, sometimes they moved in the opposite direction during the recording session. This could be an issue since place cells appear to be unidirectional on a linear track while in a 2D environment, they fire in the same place regardless of which direction the animal is facing. The rectangular track used in this study is possibly more similar to the linear track than 2D environment; hence, direction of animal's movement might have influenced the firing pattern of place cells.

4.2.5 Data analysis

The place cells were not quantitatively identified before the stimulation due to time restriction as the stimulation needed to be conducted nearly immediately after a place cell was identified. Pyramidal cells that are spatially tuned comprise ∼20 - 50% of the CA1, while the rest are either inhibitory or silent cells (Thompson and Best 1989; Wilson and McNaughton 1993; Karlsson and Frank 2008); thus, most of the recorded cells can with certain reliability be identified as place cells by subjective assessment of rate maps, spike-trajectory maps, correlograms and number of spikes during single recording session.

Spike sorting was conducted semi-automatically. Using automatic KiloSort2 spike sorter, a lot of time was saved, and it gave the opportunity to start stimulation session almost immediately after detecting a place cell. After all the experiments were conducted, the units sorted by KiloSort2 were further manually inspected removing noise, merging the same units or splitting one unit that contained different clusters. A disadvantage of using these spike sorters is that it still does not yield sorted units that doesn't require any further input. Even though it can be further analysed manually, it can be difficult to spot the same units that have been split during spike sorting. In the near future, it could be possible to use more than one spike sorter, such as Klusta (Rossant et al. 2016), IronClust (Jun et al. 2017a) and Mountainsort4 (Chung et al. 2017) and use the consensus between them in order to avoid manual curation; however, this approach needs further testing (Buccino et al. 2019).

Due to time restriction, a small sample size of stimulated place cells was acquired. Additionally, some of the recordings were corrupted rendering it inaccessible for processing. Further studies are needed to increase the dataset, and do the quantitative analysis to test if our preliminary results are representative.

4.3 The effect of extracellular stimulation on CA1 place cells

4.3.1 Changes in spatial firing in already formed place cells

As presented in the results, different outcomes of the localized stimuli were observed in spatial firing (Fig. 3.18). Significantly increased spatial correlation between cells' putative place fields and the stimulus location (spatial correlation STIM) with concomitant significant decrease in spatial correlation between cells' putative place fields and the original place field (spatial correaltion PRE), is an indicator that the extracellular stimulation can cause biased firing activity to the stimulus location. These results are in accordance with the findings from Diamantaki et al. (2018) that utilized juxtacellular stimulation in freely moving mice, a method which provides a more precise single-cell targeting.

Most of the cells (11 out of 15, ∼73%) appeared to be affected by the extracellular stimulation while in another study that utilized juxtacellular stimulation, ∼45% place cells had changed their spatial firing. Out of these 11 mentioned cells, 2 (∼13%) place cells exhibited remapping of the place fields to the targeted area and nearly completely ceased to fire at the original place field. The other 9 cells (60%) exhibited a significant increase in sparseness, displaying a

more diffused spatial firing; however, by visual inspection of rate maps, 5 out of those 9 cells did show preference for the stimulus location. Out of 15 cells analysed, 4 (∼27%) were sorted as the cells that were not significantly affected by the stimulation.

This result resembles partial remapping. In number of studies it was found that in the CA1 subfield, mostly partial remapping is present, while the CA3 subfield is more characteristic of rate and global remapping (Gothard et al.; Skaggs and McNaughton 1998; Tanila 1999; Leutgeb et al. 2004; Leutgeb et al. 2005); however, whole population of neurons (all neurons on the same tetrode for corresponding stimulation sessions) needs to be examined in order to determine what type of remapping it is.

The rapid remapping presented in CA1 place cells supports the notion of orthogonal maps' formation (Colgin et al. 2008), which in turn satisfies the need for large memory storage capacity.

The dendritic plateau potential in CA1 pyramidal cells is produced by properly timed input from EC and CA3 (Bittner et al. 2015). These signals both modulate previously established cells and can induce new place field formation. Perhaps the influence of these conjunctive signals could explain why some of the stimulated cells were not affected by the stimulation. The relationship between the conjunctive input from EC and CA3 to CA1 and the extracellular stimulation remains to be elucidated.

Due to the main interest being in whether the place field in well established place cells was affected by the stimulation or not, the categorization of stimulated place cells was based mostly on localization of peak firing rate compared to the targeted area (stimulus location) and their putative place field. Hence, the spatial correlation STIM was the primary factor for distinguishing between different outcomes in spatial tuning.

The place cells that had increased spatial correlation STIM could still be firing at the old location, and to distinguish those that are firing only at the newly formed place field from those that fire at several different location including the targeted area, value of sparsity was the next crucial factor. Cells with increased sparseness were, therefore, categorized as units with a more diffused spatial firing. The units considered to not have been changed, would be units that do not exhibit a large change in neither spatial correlation STIM, sparseness nor in selectivity. The rate maps of all 15 cells are visually in accordance with this categorization, which was also confirmed with Wilcoxon signed-rank test as expected.

Absence of significant change in average firing rate, as well as maximum firing rate, for all the stimulated cells is in agreement with the previous observation that the place fields have remapped, i.e., spatial firing was redistributed, rather than that extracellular stimulation induced change in level of cell's activity; which is also confirmed by Diamantaki et al. (2018).

The stability of the 4 cells that were not affected according to spatial correlation, sparsity, selectivity, and average firing rate, likely comes from the direct input from EC since impaired CA3-CA1 connection does not disturb sharp and rapid place field formation (Brun et al. 2002). In addition to that, CA3 place fields are formed at a much slower rate than place fields in CA1 pyramidal cells (Leutgeb et al. 2004) suggesting at least independent formation of spatially tuned cells in these two subfields under novel conditions. Nonetheless, the spatial tuning of cells recorded in these experiments is considered to be well

established since the animals have been trained in the same environment beforehand giving enough time for both CA1 and CA3 place cells to form stable place fields, which leaves direct input from EC to CA1 principal cells as a likely underlying cause of place field's stability.

The effects of extracellular stimulation resemble the effects of natural cue changes in the environment (Leutgeb et al. 2005).

The homosynaptic plasticity together with the concomitant depotentiation of previously established spatial activity (heterosynaptic plasticity) is perhaps the cellular mechanism behind remapping from original place field to the targeted area (Diamantaki et al. 2018).

4.3.2 Silent cells becoming active

The activation of silent cells is in accord with homosynaptic plasticity where stimulation-induced potentiation of location-specific input leads to spatial firing (Bittner et al. 2015; Diamantaki et al. 2018).

In the study where silent cells were stimulated juxtacellularly (Diamantaki et al. 2018), ∼32% of silent cells started to display spatial activity. Similar results were shown in a few other studies (Lee et al. 2012; Bittner et al. 2017).

In our case, there was an increase in number of recorded cells by ∼23% after the stimulation compared to before, and the place cells recorded after the stimulation had an increase in spatial correlation in reference to the stimulus location. Even though similar results were previously reported for individual silent cells, this is an indicator that the extracellular stimulation might not be as localized as desired; however, if the current was weaker, the stimulation effect might have been more localized.

4.4 Long-term observation of extracellular stimulation effects in CA1

Although the different studies reported consistent results with the data acquired in this thesis (Bittner et al. 2017; Diamantaki et al. 2018), in the other studies they were able to observe place field remapping only shortly after the stimulation sessions. The question remains, do the place cells remap permanently or just temporarily and for how long?

We attempted to find the answer to this question. The electrodes (in groups of tetrodes) on the microdrive, that are implanted and well cemented to the rat's head, tend to be quite stable. This allows the researches to record and observe single-units' activity in a course of at least a few days (also reported in Brun et al. 2002).

There were 4 different place cells observed in multiple recordings acquired over the course of 1-2 days. There were cells that either started firing diffusely, and then regained the original place field post-stimulation (Fig. 3.17), or the cell fired in both the original place field and targeted location, but afterwards continued to fire only in the original place field (Fig. 3.16).

There was another cell that was stimulated in three stimulation sessions with baseline Open-Ephys recordings in between each stimulation session (Fig. 3.15); however, only short-term place field remapping to stimulus location (regaining original place field after STIM or POST1) was observed. Following this, it

regained its original place field. The second stimulation induced diffused spatial firing after which the cell most likely disappeared. The cells were rather resistant against long-term remapping. They either fired more diffusely or did not change their original place field in post-stimulation sessions.

As in the case of resistance in short-term place field remapping immediately after (or even during) the stimulation, the reason behind stable spatial firing and resistance in long-term remapping is perhaps the input coming from the EC (Brun et al. 2002; Fyhn et al. 2007) either through perforant pathway (Andersen et al. 1971; Amaral and Witter 1989) or through direct projections to CA1 (Brun et al. 2002). The origin of these inputs that stabilize the place cell firing in CA1 could either be in other spatially tuned cells such as grid cells in MEC (Fyhn et al. 2007), or in non-spatially tuned cells from LEC (Tamamaki and Nojyo 1995; Witter et al. 2000; Naber et al. 2001).

There is evidence for underlying molecular mechanisms behind short-term and long-term stability of place fields. The short-term stability of newly formed place field is independent of NMDA receptors (Kentros et al. 1998. Long-term stability, on the other hand, appears to be dependent on functional NMDA receptors suggesting that this form of stability might be related to LTP (Kentros et al. 1998). This is to a certain extent in accordance with our results. The place fields were remapped only briefly (∼20-40 minutes after stimulation), after which the place cells regained their original place field.

There was one cell that was sorted as a place cell that remapped after the stimulation. It was observed over a course of ∼50h. Purely by subjective visual inspection of the rate maps, the remapped place field remained at the stimulus location during the entire time that it was tracked (Fig. 3.14). This suggests that there is a possibility for long-term place field remapping after only single stimulation session.

The cell that retained its place field at the stimulus location was recorded from the CA1 in the right hemisphere while the other 3 were recorded from CA1 in the left hemisphere. It was reported in humans that the right hemisphere is recruited in any kind of topographic stimulation in contrast to semantic nontopographic information recall (Maguire et al. 1997); however, these are different organisms in addition to a quite small sample size to be able to deduce any strong conclusions.

4.5 Future perspectives

There is more left to investigate with the data acquired in this thesis. For instance, spatial correlation to original place field in pre-stimulation and post-stimulation conditions for all the units recorded on the same channel group that conducts stimulation signals to investigate the possibility of global remapping. It remains to be investigated how LFP, or more precisely theta oscillations, might have been affected by the extracellular stimulation; additionally, how important phase precision of the stimulus is for the place cell remapping. The answer to different stimulation effects might lie in its timing in relation to theta oscillations. Quantified observation of place field size for comparison between pre-stimulation and post-stimulation trials could provide further insight into extracellular stimulation effects.

To ensure validity of the findings in this thesis, more data should be acquired as the data sample presented here is comparably small.

The second part of this thesis that is left incomplete is the eight-track experimental setup. Similarly to T-based decision tasks, the remarks of decision-making processes could be further investigated using the eight track. The animals would first be trained to alternate turns each time they are in the central stem (moving in eight-shape). When a place cell is detected with the place field in the central stem, its activity can be observed (firing rate and local field potential around it) and determined if there is a link between its activity and planned movement. Finally, it would be interesting to test whether the extracellular stimulation of the cell can alter animal's movement to establish the cellular mechanism behind the decision-making process in the hippocampus. Firstly, the analysis pipeline needs to be established for extracting and distinguishing data from different laps (left and right turns). As it was shown that the rate of place cell firing can encode the intended destination (Johnson and Redish 2007; Ainge et al. 2012), eight-track setup could be used to investigate whether the decision making process could be manipulated with closed-loop extracellular stimulation.

The next step could be to investigate whether the place cells more upstream of CA1, such as CA3, could be manipulated by the extracellular stimulation, how the recurrent network could be effected by it, and to which degree in comparison to CA1 place cells.

4.6 Conclusion

The preliminary results presented are promising. It was shown that biased spatial activity can be induced via extracellular stimulation in accordance with other studies that utilized different methods. This procedure is less time demanding compared to single-cell stimulation, while allowing recording multiple neurons concomitantly. Furthermore, we were able to observe long-term stimulation effects in the course of a few days, which was not achieved so far.

Stimulated cells showed significant increase in spatial correlation in reference to the stimulus location, while concomitantly decreasing spatial correlation in reference to the original place field. Since neither the maximum nor average firing rate was significantly changed, the place fields are considered to only have redistributed to the targeted area; however, stimulation effects remain to be elucidated for the whole neural population recorded on the tetrodes that conducted the stimulation current in order to assess the type of remapping. Regarding the targeted cells whose activity was tracked, not all the cells remapped to the exact location of stimulus; some were left unchanged according to spatial correlation, sparsity and selectivity, while some displayed diffused spatial firing, i.e., increase in sparseness. An overall increase in the number of cells after all the stimulation sessions indicates that silent cells, which were not targeted by the extracellular stimulation, became active. Additionally, all cells that were recorded on the same tetrode, which conducted the stimulation current showed overall increase in spatial correlation in reference to the stimulus location.

5. References

Abbott, L. F. and Nelson, S. B. (2000). Synaptic plasticity: taming the beast. *Nature neuroscience*, 3(11s):1178.

Aghajan, Z. M., Acharya, L., Moore, J. J., Cushman, J. D., Vuong, C., and Mehta, M. R. (2015). Impaired spatial selectivity and intact phase precession in two-dimensional virtual reality. *Nature neuroscience*, 18(1):121.

Ainge, J. A., Tamosiunaite, M., Wörgötter, F., and Dudchenko, P. A. (2012). Hippocampal place cells encode intended destination, and not a discriminative stimulus, in a conditional t-maze task. *Hippocampus*, 22(3):534–543.

Amaral, D. G. and Witter, M. P. (1989). The three-dimensional organization of the hippocampal formation: a review of anatomical data. *Neuroscience*, 31(3):571–591.

Andersen, P., Bliss, T., and Skrede, K. K. (1971). Lamellar organization of hippocampal excitatory pathways. *Experimental brain research*, 13(2):222–238.

Aronov, D. and Tank, D. W. (2014). Engagement of neural circuits underlying 2d spatial navigation in a rodent virtual reality system. *Neuron*, 84(2):442–456.

Barry, C., Hayman, R., Burgess, N., and Jeffery, K. J. (2007). Experience-dependent rescaling of entorhinal grids. *Nature neuroscience*, 10(6):682.

Battaglia, F. P., Sutherland, G. R., and McNaughton, B. L. (2004). Local sensory cues and place cell directionality: additional evidence of prospective coding in the hippocampus. *Journal of Neuroscience*, 24(19):4541–4550.

Bittner, K. C., Grienberger, C., Vaidya, S. P., Milstein, A. D., Macklin, J. J., Suh, J., Tonegawa, S., and Magee, J. C. (2015). Conjunctive input processing drives feature selectivity in hippocampal ca1 neurons. *Nature neuroscience*, 18(8):1133.

Bittner, K. C., Milstein, A. D., Grienberger, C., Romani, S., and Magee, J. C. (2017). Behavioral time scale synaptic plasticity underlies ca1 place fields. *Science*, 357(6355):1033–1036.

Bliss, T. V. and Lømo, T. (1973). Long-lasting potentiation of synaptic transmission in the dentate area of the anaesthetized rabbit following stimulation of the perforant path. *The Journal of physiology*, 232(2):331–356.

Boyden, E. S., Zhang, F., Bamberg, E., Nagel, G., and Deisseroth, K. (2005). Millisecond-timescale, genetically targeted optical control of neural activity. *Nature neuroscience*, 8(9):1263.

Brun, V. H., Otnæss, M. K., Molden, S., Steffenach, H.-A., Witter, M. P., Moser, M.-B., and Moser, E. I. (2002). Place cells and place recognition maintained by direct entorhinal-hippocampal circuitry. *Science*, 296(5576):2243–2246.

Buccino, A. P., Hurwitz, C. L., Magland, J., Garcia, S., Siegle, J. H., Hurwitz, R., and Hennig, M. H. (2019). Spikeinterface, a unified framework for spike sorting. *BioRxiv*, page 796599.

Buccino, A. P., Lepperød, M. E., Dragly, S.-A., Häfliger, P., Fyhn, M., and Hafting, T. (2018). Open source modules for tracking animal behavior and closed-loop stimulation based on open ephys and bonsai. *Journal of neural engineering*, 15(5):055002.

Cappaert, N. L., Van Strien, N. M., and Witter, M. P. (2015). Hippocampal formation. In *The rat nervous system*, pages 511–573. Elsevier.

Chen, G., King, J. A., Burgess, N., and O'Keefe, J. (2013a). How vision and movement combine in the hippocampal place code. *Proceedings of the National Academy of Sciences*, 110(1):378–383.

Chen, J.-Y., Lonjers, P., Lee, C., Chistiakova, M., Volgushev, M., and Bazhenov, M. (2013b). Heterosynaptic plasticity prevents runaway synaptic dynamics. *Journal of Neuroscience*, 33(40):15915–15929.

Chen, L. L., Lin, L.-H., Green, E. J., Barnes, C. A., and McNaughton, B. L. (1994). Head-direction cells in the rat posterior cortex. *Experimental Brain Research*, 101(1):8–23.

Chistiakova, M., Bannon, N. M., Bazhenov, M., and Volgushev, M. (2014). Heterosynaptic plasticity: multiple mechanisms and multiple roles. *The Neuroscientist*, 20(5):483–498.

Chung, J. E., Magland, J. F., Barnett, A. H., Tolosa, V. M., Tooker, A. C., Lee, K. Y., Shah, K. G., Felix, S. H., Frank, L. M., and Greengard, L. F. (2017). A fully automated approach to spike sorting. *Neuron*, 95(6):1381–1394.

Colgin, L. L., Leutgeb, S., Jezek, K., Leutgeb, J. K., Moser, E. I., McNaughton, B. L., and Moser, M.-B. (2010). Attractor-map versus autoassociation based attractor dynamics in the hippocampal network. *Journal of neurophysiology*, 104(1):35–50.

Colgin, L. L., Moser, E. I., and Moser, M.-B. (2008). Understanding memory through hippocampal remapping. *Trends in neurosciences*, 31(9):469–477.

Cowley, A. et al. (2011). A healthy future: platinum in medical applications. *Platinum Metals Review*, 55(2):98–107.

Deisseroth, K. (2011). Optogenetics. *Nature methods*, 8(1):26.

Diamantaki, M., Coletta, S., Nasr, K., Zeraati, R., Laturnus, S., Berens, P., Preston-Ferrer, P., and Burgalossi, A. (2018). Manipulating hippocampal place cell activity by single-cell stimulation in freely moving mice. *Cell reports*, 23(1):32–38.

Dombeck, D. A., Graziano, M. S., and Tank, D. W. (2009). Functional clustering of neurons in motor cortex determined by cellular resolution imaging in awake behaving mice. *Journal of Neuroscience*, 29(44):13751–13760.

Dombeck, D. A., Harvey, C. D., Tian, L., Looger, L. L., and Tank, D. W. (2010). Functional imaging of hippocampal place cells at cellular resolution during virtual navigation. *Nature neuroscience*, 13(11):1433.

Dombeck, D. A., Khabbaz, A. N., Collman, F., Adelman, T. L., and Tank, D. W. (2007). Imaging large-scale neural activity with cellular resolution in awake, mobile mice. *Neuron*, 56(1):43–57.

Dragly, S.-A., Hobbi Mobarhan, M., Lepperød, M. E., Tennøe, S., Fyhn, M., Hafting, T., and Malthe-Sørenssen, A. (2018). Experimental directory structure (exdir): An alternative to hdf5 without introducing a new file format. *Frontiers in neuroinformatics*, 12:16.

Dudek, S. M., Alexander, G. M., and Farris, S. (2016). Rediscovering area ca2: unique properties and functions. *Nature Reviews Neuroscience*, 17(2):89.

Elliott, T. and Shadbolt, N. R. (2002). Multiplicative synaptic normalization and a nonlinear hebb rule underlie a neurotrophic model of competitive synaptic plasticity. *Neural computation*, 14(6):1311–1322.

Ferguson, J. E., Boldt, C., and Redish, A. D. (2009). Creating low-impedance tetrodes by electroplating with additives. *Sensors and Actuators A: Physical*, 156(2):388–393.

Finelli, L. A., Haney, S., Bazhenov, M., Stopfer, M., and Sejnowski, T. J. (2008). Synaptic learning rules and sparse coding in a model sensory system. *PLoS computational biology*, 4(4):e1000062.

Fyhn, M., Hafting, T., Treves, A., Moser, M.-B., and Moser, E. I. (2007). Hippocampal remapping and grid realignment in entorhinal cortex. *Nature*, 446(7132):190.

Fyhn, M., Molden, S., Witter, M. P., Moser, E. I., and Moser, M.-B. (2004). Spatial representation in the entorhinal cortex. *Science*, 305(5688):1258–1264.

Gothard, K. M., Skaggs, W. E., and McNaughton, B. L. (1996a). Dynamics of mismatch correction in the hippocampal ensemble code for space: interaction between path integration and environmental cues. *Journal of Neuroscience*, 16(24):8027–8040.

Gothard, K. M., Skaggs, W. E., Moore, K. M., and McNaughton, B. L. (1996b). Binding of hippocampal ca1 neural activity to multiple reference frames in a landmark-based navigation task. *Journal of Neuroscience*, 16(2):823–835.

Grienberger, C., Milstein, A. D., Bittner, K. C., Romani, S., and Magee, J. C. (2017). Inhibitory suppression of heterogeneously tuned excitation enhances spatial coding in ca1 place cells. *Nature neuroscience*, 20(3):417.

Hafting, T., Fyhn, M., Molden, S., Moser, M.-B., and Moser, E. I. (2005). Microstructure of a spatial map in the entorhinal cortex. *Nature*, 436(7052):801.

Hartley, T., Burgess, N., Lever, C., Cacucci, F., and O'Keefe, J. (2000). Modeling place fields in terms of the cortical inputs to the hippocampus. *Hippocampus*, 10(4):369–379.

Hatanpaa, K. J., Raisanen, J. M., Herndon, E., Burns, D. K., Foong, C., Habib, A. A., and White III, C. L. (2014). Hippocampal sclerosis in dementia, epilepsy, and ischemic injury: differential vulnerability of hippocampal subfields. *Journal of Neuropathology & Experimental Neurology*, 73(2):136–142.

Hebb, D. (1949). *Organization of behavior*. New York: Wiley.

Hjornevik, T., Leergaard, T. B., Darine, D., Moldestad, O., Dale, A. M., Willoch, F., and Bjaalie, J. G. (2007). Three-dimensional atlas system for mouse and rat brain imaging data. *Frontiers in Neuroinformatics*, 1:4.

Ishizuka, N., Weber, J., and Amaral, D. G. (1990). Organization of intrahippocampal projections originating from ca3 pyramidal cells in the rat. *Journal of comparative neurology*, 295(4):580–623.

Jeffery, K. J., Donnett, J. G., Burgess, N., and O'Keefe, J. M. (1997). Directional control of hippocampal place fields. *Experimental Brain Research*, 117(1):131–142.

Jeffery, K. J. and O'Keefe, J. M. (1999). Learned interaction of visual and idiothetic cues in the control of place field orientation. *Experimental Brain Research*, 127(2):151–161.

Johnson, A. and Redish, A. D. (2007). Neural ensembles in ca3 transiently encode paths forward of the animal at a decision point. *Journal of Neuroscience*, 27(45):12176–12189.

Jun, J. J., Mitelut, C., Lai, C., Gratiy, S., Anastassiou, C., and Harris, T. D. (2017a). Real-time spike sorting platform for high-density extracellular probes with ground-truth validation and drift correction. *bioRxiv*, page 101030.

Jun, J. J., Steinmetz, N. A., Siegle, J. H., Denman, D. J., Bauza, M., Barbarits, B., Lee, A. K., Anastassiou, C. A., Andrei, A., Aydın, Ç., et al. (2017b). Fully integrated silicon probes for high-density recording of neural activity. *Nature*, 551(7679):232.

Jung, M. W., Wiener, S. I., and McNaughton, B. L. (1994). Comparison of spatial firing characteristics of units in dorsal and ventral hippocampus of the rat. *Journal of Neuroscience*, 14(12):7347–7356.

Kant, I. (1855). *Critique of pure reason, tr. by JMD Meiklejohn*. London: Henry George Bohn.

Kanter, B. R., Lykken, C. M., Avesar, D., Weible, A., Dickinson, J., Dunn, B., Borgesius, N. Z., Roudi, Y., and Kentros, C. G. (2017). A novel mechanism for the grid-to-place cell transformation revealed by transgenic depolarization of medial entorhinal cortex layer ii. *Neuron*, 93(6):1480–1492.

Karlsson, M. P. and Frank, L. M. (2008). Network dynamics underlying the formation of sparse, informative representations in the hippocampus. *Journal of Neuroscience*, 28(52):14271–14281.

Kentros, C., Hargreaves, E., Hawkins, R. D., Kandel, E. R., Shapiro, M., and Muller, R. V. (1998). Abolition of long-term stability of new hippocampal place cell maps by nmda receptor blockade. *Science*, 280(5372):2121–2126.

Kentros, C. G., Agnihotri, N. T., Streater, S., Hawkins, R. D., and Kandel, E. R. (2004). Increased attention to spatial context increases both place field stability and spatial memory. *Neuron*, 42(2):283–295.

Kjelstrup, K. B., Solstad, T., Brun, V. H., Hafting, T., Leutgeb, S., Witter, M. P., Moser, E. I., and Moser, M.-B. (2008). Finite scale of spatial representation in the hippocampus. *Science*, 321(5885):140–143.

Kjonigsen, L. J., Leergaard, T. B., Witter, M. P., and Bjaalie, J. G. (2011). Digital atlas of anatomical subdivisions and boundaries of the rat hippocampal region. *Frontiers in neuroinformatics*, 5:2.

Kjonigsen, L. J., Lillehaug, S., Bjaalie, J. G., Witter, M. P., and Leergaard, T. B. (2015). Waxholm space atlas of the rat brain hippocampal region: three-dimensional delineations based on magnetic resonance and diffusion tensor imaging. *Neuroimage*, 108:441–449.

Knierim, J. J. (2002). Dynamic interactions between local surface cues, distal landmarks, and intrinsic circuitry in hippocampal place cells. *Journal of Neuroscience*, 22(14):6254–6264.

Komorowski, R. W., Manns, J. R., and Eichenbaum, H. (2009). Robust conjunctive item–place coding by hippocampal neurons parallels learning what happens where. *Journal of Neuroscience*, 29(31):9918–9929.

Lee, D., Lin, B.-J., and Lee, A. K. (2012). Hippocampal place fields emerge upon single-cell manipulation of excitability during behavior. *Science*, 337(6096):849–853.

Lee, I., Yoganarasimha, D., Rao, G., and Knierim, J. J. (2004). Comparison of population coherence of place cells in hippocampal subfields ca1 and ca3. *Nature*, 430(6998):456.

Lein, E. S., Zhao, X., and Gage, F. H. (2004). Defining a molecular atlas of the hippocampus using dna microarrays and high-throughput in situ hybridization. *Journal of Neuroscience*, 24(15):3879–3889.

Leutgeb, S., Leutgeb, J. K., Barnes, C. A., Moser, E. I., McNaughton, B. L., and Moser, M.-B. (2005). Independent codes for spatial and episodic memory in hippocampal neuronal ensembles. *Science*, 309(5734):619–623.

Leutgeb, S., Leutgeb, J. K., Treves, A., Moser, M.-B., and Moser, E. I. (2004). Distinct ensemble codes in hippocampal areas ca3 and ca1. *Science*, 305(5688):1295–1298.

Lever, C., Burton, S., Jeewajee, A., O'Keefe, J., and Burgess, N. (2009). Boundary vector cells in the subiculum of the hippocampal formation. *Journal of Neuroscience*, 29(31):9771–9777.

Lynch, G. S., Dunwiddie, T., and Gribkoff, V. (1977). Heterosynaptic depression: a postsynaptic correlate of long-term potentiation. *Nature*, 266(5604):737.

Maguire, E. A., Frackowiak, R. S., and Frith, C. D. (1997). Recalling routes around london: activation of the right hippocampus in taxi drivers. *Journal of neuroscience*, 17(18):7103–7110.

Mankin, E. A., Diehl, G. W., Sparks, F. T., Leutgeb, S., and Leutgeb, J. K. (2015). Hippocampal ca2 activity patterns change over time to a larger extent than between spatial contexts. *Neuron*, 85(1):190–201.

Manns, J. R. and Eichenbaum, H. (2006). Evolution of declarative memory. *Hippocampus*, 16(9):795–808.

Markram, H., Lübke, J., Frotscher, M., and Sakmann, B. (1997). Regulation of synaptic efficacy by coincidence of postsynaptic aps and epsps. *Science*, 275(5297):213–215.

McKenzie, S., Huszár, R., English, D. F., Kim, K., Yoon, E., and Buzsáki, G. (2019). Preexisting hippocampal network dynamics constrain optogenetically induced place fields. *bioRxiv*, page 803577.

McNaughton, B., Barnes, C. A., Meltzer, J., and Sutherland, R. (1989). Hippocampal granule cells are necessary for normal spatial learning but not for spatially-selective pyramidal cell discharge. *Experimental brain research*, 76(3):485–496.

McNaughton, B. L., Barnes, C. A., Gerrard, J. L., Gothard, K., Jung, M. W., Knierim, J. J., Kudrimoti, H., Qin, Y., Skaggs, W., Suster, M., et al. (1996). Deciphering the hippocampal polyglot: the hippocampus as a path integration system. *Journal of Experimental Biology*, 199(1):173–185.

Mizumori, S., McNaughton, B., Barnes, C. A., and Fox, K. (1989). Preserved spatial coding in hippocampal ca1 pyramidal cells during reversible suppression of ca3c output: evidence for pattern completion in hippocampus. *Journal of Neuroscience*, 9(11):3915–3928.

Mizuseki, K. and Buzsáki, G. (2013). Preconfigured, skewed distribution of firing rates in the hippocampus and entorhinal cortex. *Cell reports*, 4(5):1010–1021.

Morris, R. G., Garrud, P., Rawlins, J. a., and O'Keefe, J. (1982). Place navigation impaired in rats with hippocampal lesions. *Nature*, 297(5868):681.

Moser, E. I., Kropff, E., and Moser, M.-B. (2008). Place cells, grid cells, and the brain's spatial representation system. *Annu. Rev. Neurosci.*, 31:69–89.

Moser, E. I., Moser, M.-B., and McNaughton, B. L. (2017). Spatial representation in the hippocampal formation: a history. *Nature neuroscience*, 20(11):1448.

Moser, M.-B., Rowland, D. C., and Moser, E. I. (2015). Place cells, grid cells, and memory. *Cold Spring Harbor perspectives in biology*, 7(2):a021808.

Muller, R. U., Bostock, E., Taube, J. S., and Kubie, J. L. (1994). On the directional firing properties of hippocampal place cells. *Journal of Neuroscience*, 14(12):7235–7251.

Muller, R. U. and Kubie, J. L. (1987). The effects of changes in the environment on the spatial firing of hippocampal complex-spike cells. *Journal of Neuroscience*, 7(7):1951–1968.

Naber, P. A., Lopes da Silva, F. H., and Witter, M. P. (2001). Reciprocal connections between the entorhinal cortex and hippocampal fields ca1 and the subiculum are in register with the projections from ca1 to the subiculum. *Hippocampus*, 11(2):99–104.

O'Keefe, J. (1976). Place units in the hippocampus of the freely moving rat. *Experimental neurology*, 51(1):78–109.

O'Keefe, J. (2014). Spatial cells in the hippocampal formation: Nobel lecture. [Nobel Media AB 2019]. Retrieved from https://www.nobelprize.org/prizes/medicine/2014/okeefe/lecture/.

O'Keefe, J. and Burgess, N. (1996). Geometric determinants of the place fields of hippocampal neurons. *Nature*, 381(6581):425.

O'Keefe, J. and Conway, D. (1978). Hippocampal place units in the freely moving rat: why they fire where they fire. *Experimental brain research*, 31(4):573–590.

O'Keefe, J. and Dostrovsky, J. (1971). The hippocampus as a spatial map: preliminary evidence from unit activity in the freely-moving rat. *Brain research*.

O'keefe, J. and Nadel, L. (1978). *The hippocampus as a cognitive map*. Oxford: Clarendon Press.

O'Keefe, J., Nadel, L., Keightley, S., and Kill, D. (1975). Fornix lesions selectively abolish place learning in the rat. *Experimental neurology*, 48(1):152–166.

O'Keefe, J. and Speakman, A. . (1987). Single unit activity in the rat hippocampus during a spatial memory task. *Experimental brain research*, 68(1):1–27.

Ólafsdóttir, H. F., Barry, C., Saleem, A. B., Hassabis, D., and Spiers, H. J. (2015). Hippocampal place cells construct reward related sequences through unexplored space. *Elife*, 4:e06063.

Pachitariu, M., Steinmetz, N., Kadir, S., Carandini, M., and Harris, K. D. (2016). Kilosort: realtime spike-sorting for extracellular electrophysiology with hundreds of channels. *BioRxiv*, page 061481.

Paxinos, G. and Watson, C. (2007). *The Rat Brain in Stereotaxic Coordinates*. Academic Press, 6 edition.

Paxinos, G., Watson, C., Pennisi, M., and Topple, A. (1985). Bregma, lambda and the interaural midpoint in stereotaxic surgery with rats of different sex, strain and weight. *Journal of neuroscience methods*, 13(2):139–143.

Pekny, M. and Nilsson, M. (2005). Astrocyte activation and reactive gliosis. *Glia*, 50(4):427–434.

Pinault, D. (1996). A novel single-cell staining procedure performed in vivo under electrophysiological control: morpho-functional features of juxtacellularly labeled thalamic cells and other central neurons with biocytin or neurobiotin. *Journal of neuroscience methods*, 65(2):113–136.

Pinault, D. (2011). The juxtacellular recording-labeling technique. In *Electrophysiological recording techniques*, pages 41–75. Springer.

Quirk, G. J., Muller, R. U., and Kubie, J. L. (1990). The firing of hippocampal place cells in the dark depends on the rat's recent experience. *Journal of Neuroscience*, 10(6):2008–2017.

Ravassard, P., Kees, A., Willers, B., Ho, D., Aharoni, D., Cushman, J., Aghajan, Z. M., and Mehta, M. R. (2013). Multisensory control of hippocampal spatiotemporal selectivity. *Science*, 340(6138):1342–1346.

Redish, A. D. and Touretzky, D. S. (1997). Cognitive maps beyond the hippocampus. *Hippocampus*, 7(1):15–35.

Ribak, C. E., Seress, L., and Amaral, D. G. (1985). The development, ultrastructure and synaptic connections of the mossy cells of the dentate gyrus. *Journal of neurocytology*, 14(5):835–857.

Rossant, C., Kadir, S. N., Goodman, D. F., Schulman, J., Hunter, M. L., Saleem, A. B., Grosmark, A., Belluscio, M., Denfield, G. H., Ecker, A. S., et al. (2016). Spike sorting for large, dense electrode arrays. *Nature neuroscience*, 19(4):634.

Russell, N. A., Horii, A., Smith, P. F., Darlington, C. L., and Bilkey, D. K. (2003). Long-term effects of permanent vestibular lesions on hippocampal spatial firing. *Journal of Neuroscience*, 23(16):6490–6498.

Samsonovich, A. and McNaughton, B. L. (1997). Path integration and cognitive mapping in a continuous attractor neural network model. *Journal of Neuroscience*, 17(15):5900–5920.

Sargolini, F., Fyhn, M., Hafting, T., McNaughton, B. L., Witter, M. P., Moser, M.-B., and Moser, E. I. (2006). Conjunctive representation of position, direction, and velocity in entorhinal cortex. *Science*, 312(5774):758–762.

Schoenenberger, P., O'Neill, J., and Csicsvari, J. (2016). Activity-dependent plasticity of hippocampal place maps. *Nature communications*, 7:11824.

Schultz, C. and Engelhardt, M. (2014). Anatomy of the hippocampal formation. In *The Hippocampus in Clinical Neuroscience*, volume 34, pages 6–17. Karger Publishers.

Scoville, W. B. and Milner, B. (1957). Loss of recent memory after bilateral hippocampal lesions. *Journal of neurology, neurosurgery, and psychiatry*, 20(1):11.

Shapiro, M. L., Tanila, H., and Eichenbaum, H. (1997). Cues that hippocampal place cells encode: dynamic and hierarchical representation of local and distal stimuli. *Hippocampus*, 7(6):624–642.

Sharp, P., Kubie, J., and Muller, R. (1990). Firing properties of hippocampal neurons in a visually symmetrical environment: contributions of multiple sensory cues and mnemonic processes. *Journal of Neuroscience*, 10(9):3093–3105.

Siegle, J. H., López, A. C., Patel, Y. A., Abramov, K., Ohayon, S., and Voigts, J. (2017). Open ephys: an open-source, plugin-based platform for multichannel electrophysiology. *Journal of neural engineering*, 14(4):045003.

Skaggs, W. E. and McNaughton, B. L. (1998). Spatial firing properties of hippocampal ca1 populations in an environment containing two visually identical regions. *Journal of Neuroscience*, 18(20):8455–8466.

Skaggs, W. E., McNaughton, B. L., and Gothard, K. M. (1993). An information-theoretic approach to deciphering the hippocampal code. In *Advances in neural information processing systems*, pages 1030–1037.

Skaggs, W. E., McNaughton, B. L., Wilson, M. A., and Barnes, C. A. (1996). Theta phase precession in hippocampal neuronal populations and the compression of temporal sequences. *Hippocampus*, 6(2):149–172.

Sloviter, R. S. and Damiano, B. P. (1981). Sustained electrical stimulation of the perforant path duplicates kainate-induced electrophysiological effects and hippocampal damage in rats. *Neuroscience letters*, 24(3):279–284.

Smith, D. M. and Mizumori, S. J. (2006). Hippocampal place cells, context, and episodic memory. *Hippocampus*, 16(9):716–729.

Solstad, T., Boccara, C. N., Kropff, E., Moser, M.-B., and Moser, E. I. (2008). Representation of geometric borders in the entorhinal cortex. *Science*, 322(5909):1865–1868.

Solstad, T., Brun, V., Kjelstrup, K., Fyhn, M., Witter, M., et al. (2007). Grid expansion along the dorso-ventral axis of the medial entorhinal cortex. In *Soc. Neurosci. Abstr*, volume 33.

Stackman, R. W., Clark, A. S., and Taube, J. S. (2002). Hippocampal spatial representations require vestibular input. *Hippocampus*, 12(3):291–303.

Swanson, L., Wyss, J., and Cowan, W. (1978). An autoradiographic study of the organization of intrahippocampal association pathways in the rat. *Journal of comparative neurology*, 181(4):681–715.

Tamamaki, N., Abe, K., and Nojyo, Y. (1987). Columnar organization in the subiculum formed by axon branches originating from single ca1 pyramidal neurons in the rat hippocampus. *Brain research*, 412(1):156–160.

Tamamaki, N. and Nojyo, Y. (1995). Preservation of topography in the connections between the subiculum, field ca1, and the entorhinal cortex in rats. *Journal of Comparative Neurology*, 353(3):379–390.

Tang, Q., Brecht, M., and Burgalossi, A. (2014). Juxtacellular recording and morphological identification of single neurons in freely moving rats. *nature protocols*, 9(10):2369.

Tanila, H. (1999). Hippocampal place cells can develop distinct representations of two visually identical environments. *Hippocampus*, 9(3):235–246.

Tanila, H., Shapiro, M. L., and Eichenbaum, H. (1997). Discordance of spatial representation in ensembles of hippocampal place cells. *Hippocampus*, 7(6):613–623.

Taube, J. S. (2007). The head direction signal: origins and sensory-motor integration. *Annu. Rev. Neurosci.*, 30:181–207.

Taube, J. S., Muller, R. U., and Ranck, J. B. (1990a). Head-direction cells recorded from the postsubiculum in freely moving rats. i. description and quantitative analysis. *Journal of Neuroscience*, 10(2):420–435.

Taube, J. S., Muller, R. U., and Ranck, J. B. (1990b). Head-direction cells recorded from the postsubiculum in freely moving rats. ii. effects of environmental manipulations. *Journal of Neuroscience*, 10(2):436–447.

Thompson, L. and Best, P. (1989). Place cells and silent cells in the hippocampus of freely-behaving rats. *Journal of Neuroscience*, 9(7):2382–2390.

Tolman, E. C. (1948). Cognitive maps in rats and men. *Psychological review*, 55(4):189.

Touretzky, D. S. and Redish, A. D. (1996). Theory of rodent navigation based on interacting representations of space. *Hippocampus*, 6(3):247–270.

Veazey, R., Amaral, D. G., and Cowan, W. (1982). The morphology and connections of the posterior hypothalamus in the cynomolgus monkey (macaca fascicularis). ii. efferent connections. *Journal of Comparative Neurology*, 207(2):135–156.

Voigts, J., Siegle, J. H., Pritchett, D. L., and Moore, C. I. (2013). The flexdrive: an ultra-light implant for optical control and highly parallel chronic recording of neuronal ensembles in freely moving mice. *Frontiers in systems neuroscience*, 7:8.

West, M. J., Coleman, P. D., Flood, D. G., and Troncoso, J. C. (1994). Differences in the pattern of hippocampal neuronal loss in normal ageing and alzheimer's disease. *The Lancet*, 344(8925):769–772.

Wilson, M. A. and McNaughton, B. L. (1993). Dynamics of the hippocampal ensemble code for space. *Science*, 261(5124):1055–1058.

Witter, M. P., Wouterlood, F. G., Naber, P. A., and Van Haeften, T. (2000). Anatomical organization of the parahippocampal-hippocampal network. *Annals of the New York Academy of Sciences*, 911(1):1–24.

Wu, F., Stark, E., Ku, P.-C., Wise, K. D., Buzsáki, G., and Yoon, E. (2015). Monolithically integrated μleds on silicon neural probes for high-resolution optogenetic studies in behaving animals. *Neuron*, 88(6):1136–1148.

Wu, Z. and Yamaguchi, Y. (2006). Conserving total synaptic weight ensures one-trial sequence learning of place fields in the hippocampus. *Neural networks*, 19(5):547–563.

Yartsev, M. M. and Ulanovsky, N. (2013). Representation of three-dimensional space in the hippocampus of flying bats. *Science*, 340(6130):367–372.

Zalutsky, R. A. and Nicoll, R. A. (1990). Comparison of two forms of long-term potentiation in single hippocampal neurons. *Science*, 248(4963):1619–1624.

Zinyuk, L., Kubik, S., Kaminsky, Y., Fenton, A., and Bures, J. (2000). Understanding hippocampal activity by using purposeful behavior: place navigation induces place cell discharge in both task-relevant and task-irrelevant spatial reference frames. *Proceedings of the National Academy of Sciences*, 97(7):3771–3776.

6. Appendix

6.1 List of abbreviations

BTSP - Behavioural time scale synaptic plasticity
CA1 - Cornu ammonis 1
CA2 - Cornu ammonis 2
CA3 - Cornu ammonis 3
DG - Dentate gyrus
DLE - Dorso-lateral entorhinal area
EC - Entorhinal cortex
FC - Fasciola cinereum
FPGA - Field-programmable gate array
GUI - Graphical user interface
HF - Hippocampal formation
IP - Intraperitoneal
LEC - Lateral entorhinal cortex
LFP - Local field potential
LTP - Long-term potentiation
MEC - Medial entorhinal cortex
NMDA - N-methyl-D-aspartate
OSC - Open sound control
PBS - Phosphate buffered saline
PER - Perirhinal cortex
PFA - Paraformaldehyde
SC - Subcutaneous
SPI - Serial peripheral interface
SUB - Subiculum

6.2 Solutions used for histology

Sucrose (Sigma-Aldrich: BioXtra, $\geq$ 99.5%)

Phosphate-buffered saline (PBS) - 10X PBS

- 80g $NaCl$
- 2.0g KCl
- 14.4g Na_2HPO_4
- 2.4g KH_2PO_4

Protocol:

1. Dissolve in 800 ml dH_2O.
2. Adjust pH to 7.4.
3. Adjust volume to 1L.

To get 1X solution, 10x PBS is diluted 1:10 (100ml 10X PBS + 900ml dH_2O).

4% paraformaldehyde (PFA)

- 40g PFA
- 1L 1X PBS

Protocol:

1. Heat to 50-60°C.
2. Stir until everything is dissolved (3-4 hours)
3. Filter before use.

Cresyl violet staining solution

- 0.5g cresyl violet acetate
- 1.25 mL glacial acetic acid
- 500 mL dH_2O

Protocol:

1. Heat to 60°C
2. Filter.

Other solutions used for staining of Nissl bodies:

- 70% ethanol
- 80% ethanol
- 90% ethanol

- 96% ethanol with acetic acid (Acetic acid - Sigma-Aldrich, ReagentPlus®: $\geq$ 99%)
- absolute ethanol
- xylene (VWR International, BDH®: mixture of isomers xylène, xylol, xyleen, xilene, xylen)
- entellan (Merck KGaA: contains mixture of xylene isomers)

Alcohol solutions are made by diluting the absolute ethanol solution with dH_2O.

6.3 Protocol for histology

Staining for Nissl bodies
Everything is done under the fume hood. Sometimes Part 1 can be skipped if the sections are mounted on the slides firm enough.

Part 1
Before starting, the slides need to be left to dry for at least 24 hours. After that, submerge sections in a glass container with:

1. 1:1 Absolute ethanol:Chloroform over night
2. absolute ethanol for 1.5 - 2 min
3. 90% ethanol for 1.5 - 2 min
4. 80% ethanol for 1.5 - 2 min
5. 70% ethanol for 1.5 - 2 min

Part 2
Immediately after Part 1, or if skipped start by submerging the slides into a glass container with:

1. dH_2O briefly (up to 1 min)
2. cresyl violet for 6-10 min (depending on the sections and how fresh the solution is; until the sections obtain dark blue colour
3. dH_2O briefly
4. 70% ethanol for 30 sec - 1.5 min (depending on how quickly the colour is washed away)
5. 80% ethanol for 30 sec - 1.5 min
6. 90% ethanol for 30 sec - 1.5 min
7. 96% ethanol with acetic acid
8. absolute ethanol for 30 sec - 1.5 min
9. xylene for 2 min

Slides can stay in xylene while microscope cover glasses (24 x 60 mm) are put onto the other slides. For each slide:

1. apply a few drops of entellan
2. apply the cover glass from one end to the other starting a bit lower than it is suppose to be and press gently onto the cover glass and moving the slide downwards
3. submerge the slide briefly inyo xylene to remove excess entellan on the slide
4. place upright to dry over night

6.4 Research animals and experiments

Table 8.4.1. Information on all the research animals that were used for both pilot and full scale experiments

Animal ID	Sex	Age (months) *	mass (g)	Implants	Training **	Purpose
1824	male	7	635	HC bilateral	2 weeks	Pilot
1826	male	7	473	HC bilateral	2 weeks	Pilot
1828	male	7	550	HC bilateral	2 weeks	Pilot
0006	male	3	360	HC bilateral	1 month	Full scale
0007	male	3	360	HC bilateral	1 month	Full scale
0008	male	3	360	HC bilateral	1 month	Full scale
0009	male	3	365	HC bilateral	1 month	Full scale

* age at which the experiments have started
** duration of the training before the experiments started

6.5 Implantation coordinates

Table 8.5.1. Coordinates for microdrive implantation on animals that were used for both pilot and full scale experiments

	Microdrive							
	Left hemisphere (mm)				Right hemisphere (mm)			
Animal ID	B/S *	ML **	DV ***	angle (°)	B/S	ML	DV	angle (°)
1824	B - 4.00	- 3.10	1.80	0	B - 4.00	3.10	1.80	0
1826	B - 4.00	- 3.10	1.80	0	B - 4.00	3.10	1.80	0
1828	B - 4.00	- 3.10	1.80	0	B - 4.00	3.10	1.80	0
0006	B - 4.00	- 3.10	1.80	0	B - 4.00	3.10	1.80	0
0007	B - 4.02	- 3.02	1.80	0	B - 4.00	3.10	1.80	0
0008	B - 4.00	- 3.10	1.80	0	B - 4.00	3.10	1.80	0
0009	B - 4.00	- 3.10	1.80	0	B - 4.00	3.10	1.80	0

* B - bregma, S - transverse sinus
** mediolateral
*** dorsoventral

6.6 Histology results

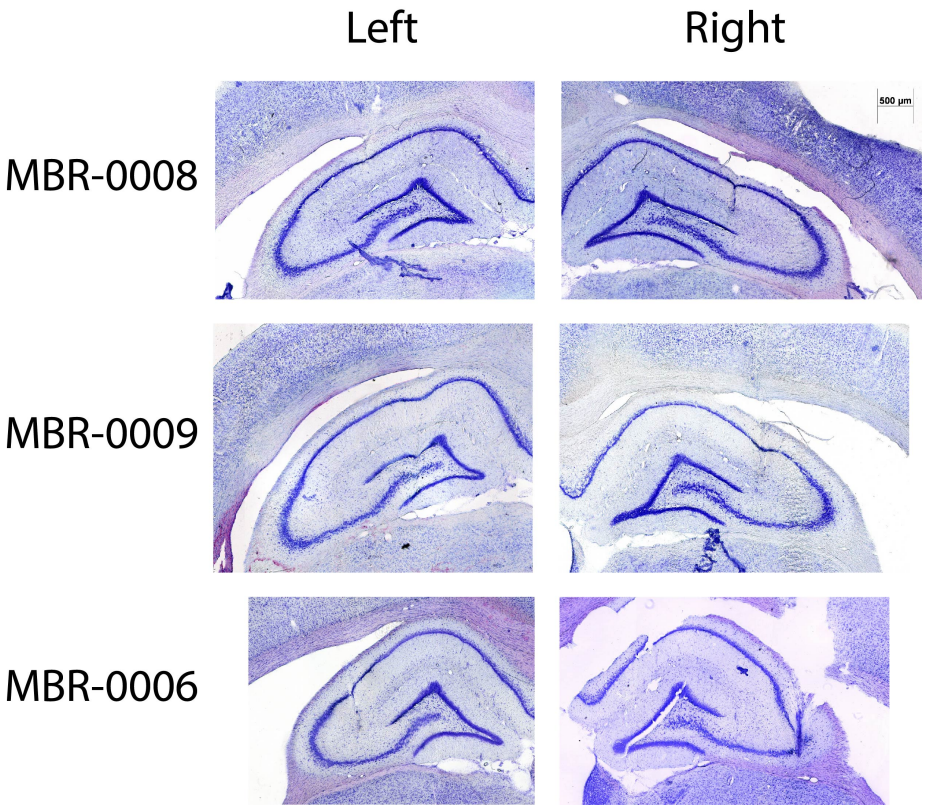

Figure 6.1: Nissl stained coronal brain sections depicting the recording sites in experimental animals.